Building and Environment 126 (2017) 221–237

Contents lists available at ScienceDirect

Building and Environment

journal homepage: www.elsevier.com/locate/buildenv

Precipitation collection and evapo(transpi)ration of living wall systems: A comparative study between a panel system and a planter box system

P.M.F. van de Wouw*, E.J.M. Ros, H.J.H. Brouwers

Department of the Built Environment, Unit Building Physics and Services, Eindhoven University of Technology, P.O. Box 513, 5600 MB Eindhoven, The Netherlands

ARTICLE INFO

Keywords:
Living wall systems
Water balance
Evapotranspiration
Precipitation collection
Evaporation model

ABSTRACT

By reducing the quantity of precipitation reaching the ground, a green façade can contribute to a more natural way of rainwater drainage. Additionally, it provides shadowing, insulation, and evapotranspiration (ET) of water enabling it to reduce the heat load of a building. The collection of precipitation and the ET were tested over a two month period on two commercially available living wall systems. The entering and outgoing amounts of water were monitored, as well as the mass variation of the systems. The weather data, collection of precipitation and condensation, and the ET were determined. The precipitation collection of one vertical m^2 expressed as an equivalent percentage of the precipitation on one horizontal m^2 results on average in 18.8% and 33.0% for the panel and the planter box system respectively, whereby the occurrence of wind driven rain is not essential. Wind speed, humidity, air temperature, and solar radiation have been found to be neither independent nor dominant, yet trends for both systems are in good correlation. Correlating the measured ET with the reference ET obtained through the FAO-56 Penman-Monteith equation results in a factor of 1.46 and 0.76 between a horizontal m^2 of reference crop and a vertical m^2 of the panel and the planter box system respectively, values relating to deviating designs and dissimilar irrigation procedures. The total estimated ET power is 18 (± 3) kW/m^2/year and 11 (± 3) kW/m^2/year for the panel and the planter box system, respectively. The derived water balances indicate the need for proper irrigation management throughout the year.

1. Introduction

The presence of vegetation in the urban environments has been shown to have many benefits, for the environment (air purification of carbon dioxide, nitrogen oxides, and particulate matter, thermal insulation, noise reduction, protection of building materials against the environment, reducing the “urban heat island” effect, improving the microclimate, improving the biodiversity) as well as for people (reducing stress levels, and an increased well-being and productivity) [1–11].

Nowadays, the artificial drainage of precipitation is needed to replace the natural drainage of former urban green areas, which have been gradually replaced by impermeable surfaces, such as streets and roofs [12–16]. The introduction of the green roof is a way of reintegrating urban green, resulting in a semi-natural form of rainwater discharge [12–15,17,18]. Like a traditional roof, the traditional façade is an impermeable surface which receives precipitation under the influence of the wind. This water runs down the façade and is discharged onto the ground or into sewers. Studies on green roofs have shown a soil substrate with plants to retain on average 60%–100% of the total precipitation [13–15,18]. Similar to green roofs, green façades have the potential to collect, retain, and gradually discharge rainwater. However, in contrast to green roofs, the quantity of rainwater collection of green façades is still unknown. Furthermore, studies which could indicate the influence of the slope on rainwater retention are indecisive, reporting it to have either a negative [13,14,19,20] or no influence on the retention of rainwater [3,18,21].

In addition to precipitation management, green façades can contribute to a comfortable indoor climate by providing shadow, insulation, and evapo(transpi)ration (ET), whereby water evaporates from the substrate and plants and transpires vapour through the plant pores. Solar radiation is absorbed and reflected by the foliage and the supporting structure, preventing it from attaining the substructure and openings [11,22–30]. Additionally, the system, covered with a dense layer of foliage, creates an air cavity, resulting in additional insulation. Varying insulation values are given in the literature, being in the range of the insulation values of double glazing [15,26,31–38]. Finally, the green façade evapo(transpi)rates water, herewith consuming 2.45 MJ/kg (at 20 °C) of latent heat for the vaporization of water [39] and consequently cooling the surrounding area adiabatically. Many studies have shown a significant contribution of the adiabatic or evaporative

* Corresponding author.
E-mail address: p.m.f.v.d.wouw@tue.nl (P.M.F. van de Wouw).

http://dx.doi.org/10.1016/j.buildenv.2017.10.002
Received 31 July 2017; Received in revised form 21 September 2017; Accepted 1 October 2017
Available online 03 October 2017

cooling of green façade systems to their surroundings and the indoor climate [15–17,24,27,28,34,37,38,40–49]. However, research on the magnitude of evaporative cooling, specifically for modular pre-grown non-ground-based external vertical greening systems, so-called living wall systems (LWS), also known as green walls, vertical gardens, and vertical greenery systems [40,48–52], are not reported yet in the literature, to the best of the authors' knowledge.

In contrast with direct and indirect green façade systems, LWS are not exclusively limited to rooting at the base of the façade and the use of climbing vegetation, causing them to possess a far larger aesthetical and creative potential, allow for a rapid covering of extensive surfaces, and extend to higher areas [52,53]. As a consequence, due to design complexity, materials involved, and maintenance, LWS have substantially larger installation costs, life cycle costs, and environmental impact [54–56]. The most relevant benefits, from a cost-benefit point of view, are related to real estate and energy savings for air conditioning. For the latter, the application of LWS is preferred over direct or indirect green façade systems, since the presence of substrate is key in obstructing conductive heat exchange [30,49,57,58]. While social, ecological, and environmental benefits predominantly relate to a macro scale and have limited impact on the monetary value, they reduce the environmental impact [55]. The costs and emergy (a measure for directly and indirectly consumed energy needed for the creation of a product or service in line with the Odum energy systems theory [59]) of installation and maintenance services (labour, water, and nutrients) are important for both an economically and environmentally sustainable vertical greening system [60,61]. Knowledge of both energy saving ability and ideal water management is therefore needed [62].

For theoretical studies of plant evaporation, the standardised FAO-56 Penman-Monteith equation of the United Nations Food and Agriculture Organisation (hereinafter called PM equation) is typically used [39]. This equation uses a hypothetical reference crop to overcome the necessity for unique evaporation parameters for individual plant species. Through crop specific coefficients, distinct ET rates are related to the rate of ET from the reference surface (ET_o) [39]. In prior studies regarding the use of plants in double skin facades and the evaporation of vertical gardens, this equation was successfully applied [63,64]. The application of the PM equation to the ET measured in an experimental setup enables a year-round prognosis for the ET power of a green façade system, as well as the consequent potential heat load reduction on buildings.

The primary goal of this study is to determine the changes in the internal water balance of distinctly dissimilar living wall systems under the influence of prevailing weather conditions in order to provide an in-depth understanding of the incoming and outgoing quantities of water, the optimisation of irrigation management, and the possibility of a predictive estimation of the potential evaporative cooling behaviour of such a living wall system prior to application.

In this study, two commercially available living wall systems are tested during 2 months with the intent to gain more insight in the collection and retention of precipitation, evapo(transpi)ration, and the resulting conversion of solar radiation. Based on these results, a year round prognosis is proposed for the evaporative power of both systems, by making use of the PM equation. Finally, a system specific water balance is set up for the complete test period, visualising the occurring internal water flows. The knowledge gained can be used to design with green façades as contributing factors to the indoor climate with an optimised water management.

2. Materials and methods

2.1. Test location and conditions

This study took place at the Eindhoven University of Technology (TU/e), the Netherlands, for a period of 2 months (from the end of November until the end of January). This specific period is chosen because of desired test conditions, ensuring various magnitudes of precipitation events together with a wide range of wind speeds. These are best met in the early winter months for the location of Eindhoven. Representative measurements regarding the ET are ensured by using evergreen plants. Because they keep the same ground coverage year-round and do not wilt, their ET is not influenced by growing seasons [39].

During the period that both LWS have been monitored, 47 and 61 successful measurement days for the panel and the planter box system respectively were achieved before frost set in and the test had to be aborted. Fig. 1a, b, and c show the geographical location (latitude:

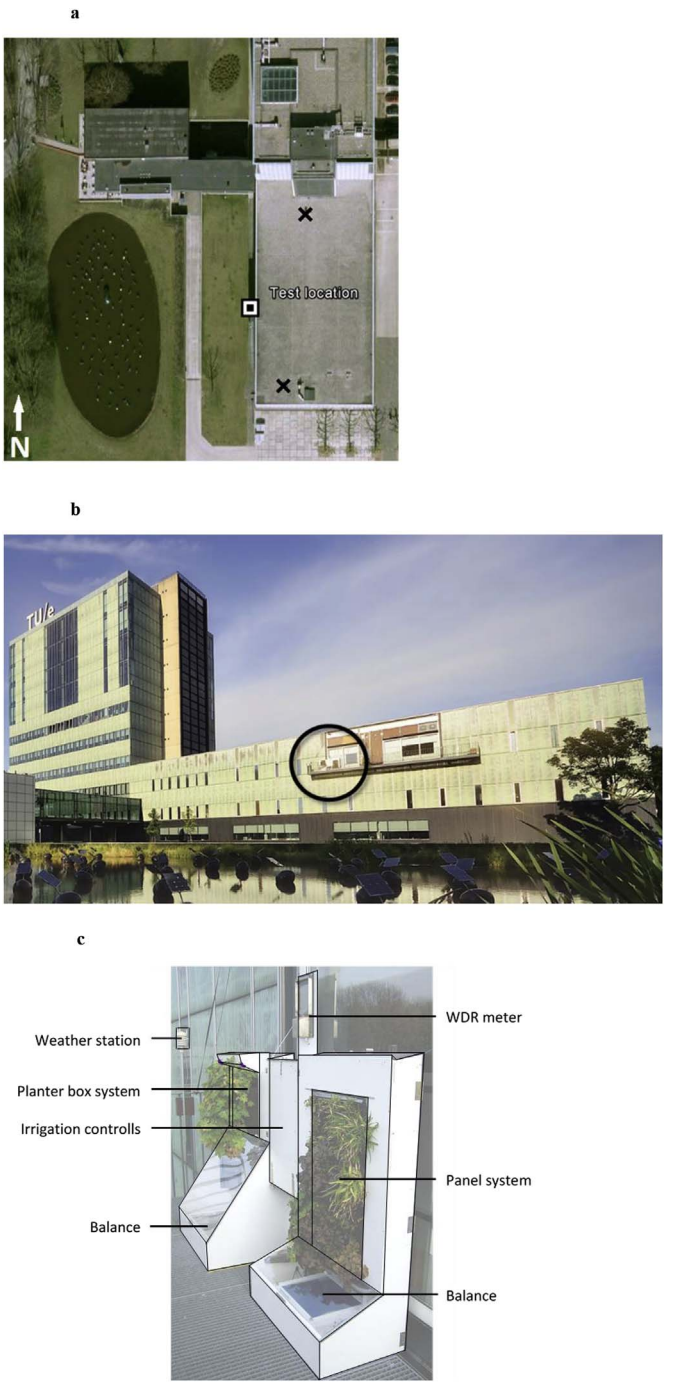

Fig. 1. Location and orientation of the test façades: a. Satellite image of the location of the test setup and the rain gauges (marked with X), b. Test setup on the west façade of the 'Vertigo' building of the Eindhoven University of Technology, the Netherlands [82], c. Test setup with the mounted panel system (right) and planter box system (left).

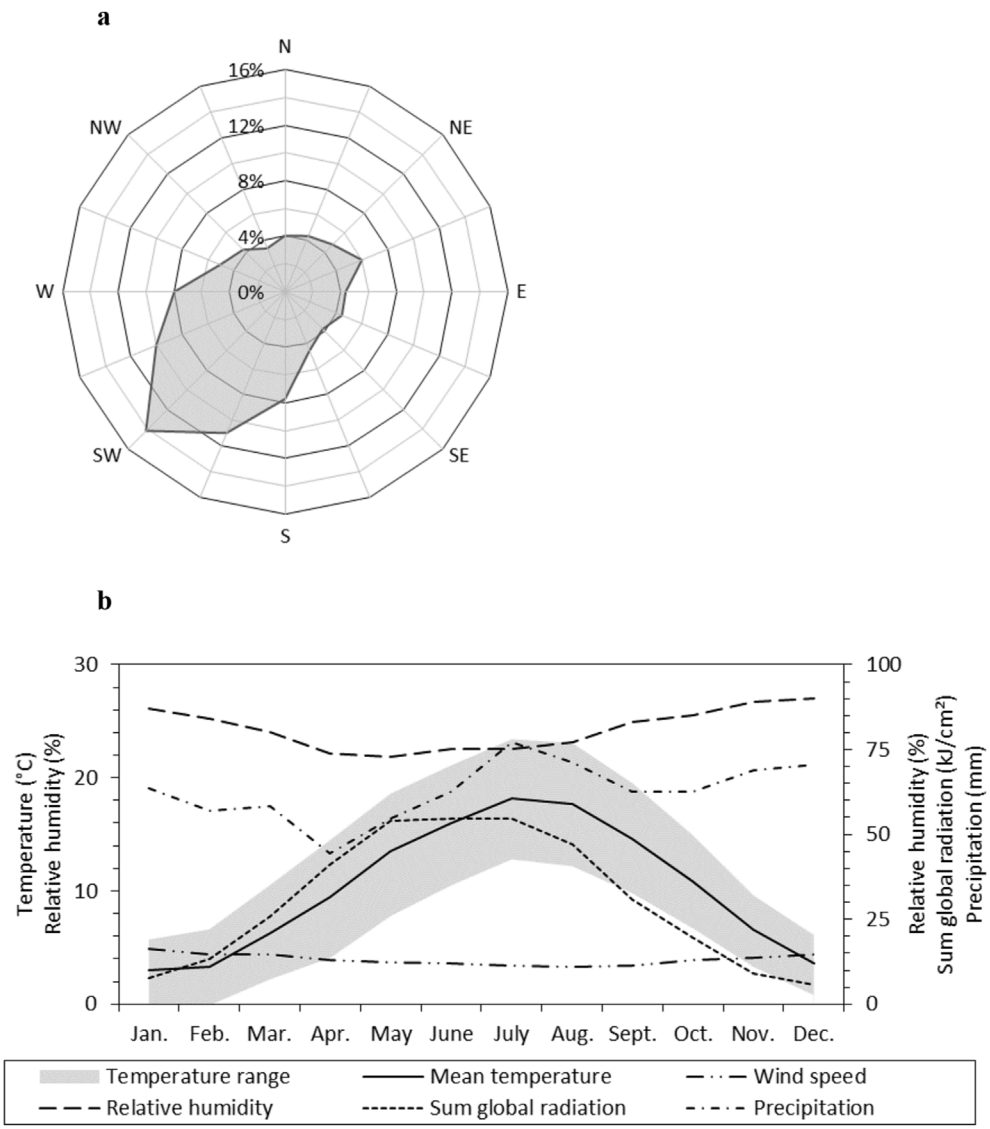

Fig. 2. Meteorological conditions for Eindhoven, the Netherlands: a. Yearly mean wind direction in percentage of time (1985–2017) [83], b. Monthly mean values for: temperature, wind speed, radiant exposure of global radiation, relative humidity, total precipitation (1981–2010) [68].

51.45, longitude: 5.48), the position of the setup on the west façade of the Vertigo building at the TU/e, and the test setup on the balcony respectively. The exact location of the experiment was carefully selected based on meteorological conditions. The predominant wind direction for Eindhoven, the Netherlands, is southwest (Fig. 2a). Hence, considering a cardinally positioned building, the test facades would be ideally facing either south or west in order to study the collection of WDR. Taking into account the heat load on a building, a west-facing façade receives direct nearly orthogonally irradiance solar radiance which is combined with a higher ambient temperature (gained during the day). Consequently, the need for a reduction of the heat load can be considered higher than for a south façade where the angle of incidence is higher [65]. In turn, the west-facing façade is selected over the south façade to perform the experiment.

Not only the climate, time of the year, and façade orientation influence the performance of a LWS, also the shape of the building and the exact position on the façade have a considerable effect on the conditions at the face of the façade. The speed and direction of the wind are influenced, as well as the quantity of rain reaching the façade. According to Blocken and Carmeliet, the maximum WDR exposure and the highest variation takes place at the top corners of a façade. The lower part of a building will receive less WDR in case the wind-blocking effect is larger [66]. To minimise the influence of these effects on the measurements, it was decided to position the LWS in front of the west façade of a medium-rise, wide building slab on the campus of the Eindhoven University of Technology. The location on the façade is chosen 30 m out of the corner of the building to prevent a corner effect. Whereas, strong (turbulent) winds in the vicinity of the edge of the roof are avoided by locating the setup 4 m lower. In front of the test setup, a large open area stretches around 180° where, 65 m to the west 3 single trees (± 20 m in height) are located, and 60 m to the south a row of trees (± 15 m in height) is situated. By choosing this location, the influence of wind is comparatively stable while a rain catch ratio in the range of 0.4–0.8 relative to the free-field conditions can theoretically be achieved [66].

According to the most used climate classification system, the Köppen-Geiger map, the test site is located in a warm temperate, fully humid, and warm summer (Cfb) climate [67]. Fig. 2b gives an overview of the expected meteorological conditions for the test location based on the monthly mean values (period 1981–2010) [68].

2.2. Living wall systems

Living Wall Systems (LWS) are available in a wide variety and many different ways of categorizations exist in the literature. Fig. 3a–d shows the typology adopted by the authors. In this study, two commercially available living wall systems (LWS) of the planter box and the panel type (Fig. 3a and b) have been investigated. These systems have been

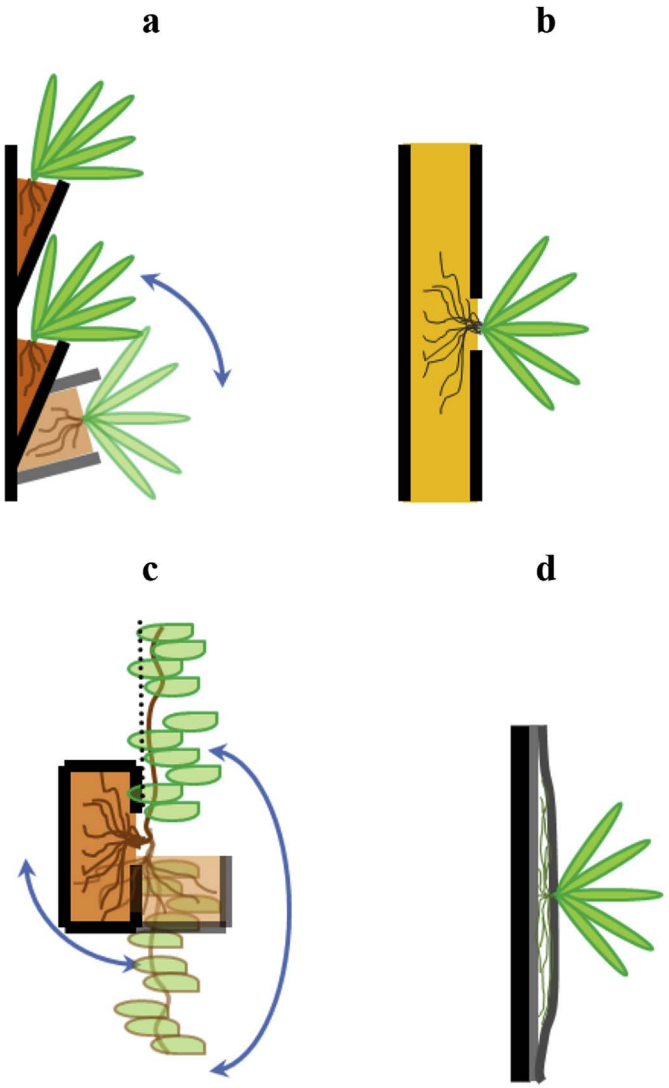

Fig. 3. LWS system typology based on: a. planter boxes filled with a growth medium, 0°–90° to the horizontal; b. enclosed or incorporated growth medium at a vertical orientation; c. planter box or panel system combined with facilities for climbing or hanging plants; d. non-biodegradable geotextile, functioning as growth medium.

chosen due to their relatively larger exposed surface area and growth medium volume in comparison with the combination system and the geotextile system (Fig. 3c and d). Inherently they, therefore, possess a higher potential for precipitation collection and buffering. Both are indirect prefabricated modular systems which are commonly mounted detached from the façade [40]. The first system is of the planter box type (Fig. 3a) which effectively measures 0,60 × 0.55 m while mounted, resulting in an effective vertical surface of 0.33 m^2 [57,69]. In this LWS, the vegetation is rooted in a horizontal potting soil medium with a volume of ± 35 l, making the system similar to that of a classic planter. The second system is a modular prefabricated hydroponic panel system fitted with mineral wool (Fig. 3b), hereinafter referred to as panel system, measuring 0,60 × 1,00 m in size it has a substrate volume of 42 l, effectively covering 0.67 m^2 of façade surface while mounted [70]. In contrast to the planter box system, the panel has a vertical surface which is covered with greenery by the insertion of pre-grown plug plants into the mineral wool substrate.

Herewith, both systems possess distinctively dissimilar growing conditions, resulting in a different plant suitability. To ensure a representative outcome regarding the performance of each system as a whole, the individual systems were planted with a diverse selection of predominantly wintergreen plant species found most successful. Hence, the dissimilarity in evapotranspiration when applying a single type of different species is to a certain extent evened out, however, it cannot be completely excluded. Prior to the test, both LWS have been pre-grown, ensuring well-rooted, healthy vegetation.

Since the plants are not rooted into the earth, the buffer for both water and nutrients is limited, making them dependent on irrigation systems. Relative to the potting soil used in the planter box system, the mineral wool of the panel system has a low buffering capacity, requiring a high irrigation frequency. For the irrigation of both systems, a pressure equalizing, self-closing, and self-cleaning commercially available irrigation system with a specified capacity of 2 l/hour was selected (Gardena micro drip). Prior to application, the inline drip heads were tested, selected, and calibrated to ensure a constant, equal, and measurable dosage of water. In consultation with the company providing the panel system, the irrigation duration and frequency have been set to 1 min every 3 h with 3 dripper heads delivering a total of 0.79 l per day. The company supplying the planter box system advised a necessity-guided irrigation at a mass loss of approximately 1.5 kg. After an initial wetting prior to the measurement period, the planter box system has only been irrigated once during the duration of the test, with an amount of 1430 ml.

2.3. Experimental design

A deviation in the mass of a LWS over time is a measure of a change in its internal water buffer. However, three categories of influencing factors can be distinguished: primary factors such as the dry weight of the LWS and added irrigation; secondary factors, in general external influences such as precipitation, evapo(transpi)ration, wind, and changes in the biomass; and tertiary factors which involve for example animals, faeces, biomass from other vegetation, falling objects, human action, fire, etc. Both primary and secondary factors are of interest; however, only primary factors can be influenced or equated for. Tertiary factors are either avoided, or their influence is accounted for. To mimic the conditions of a façade mounted system surrounded by other modules, both systems are partially enclosed avoiding the influence of tertiary factors. Hereby, the top, back, bottom, and sides are shielded from weather conditions while the front and protruding parts are exposed. In case of the planter box system, the protruding part of a module situated directly above is accounted for in the in the enclosure. To avoid an influence on the mass measurement, the systems are kept detached from their enclosure by maintaining a gap of 5 mm on all adjacent sides. Fig. 4a and b display cross-sections of the panel and the planter box system test setup, respectively.

Factors contributing to a water content increase causing a mass gain are irrigation and precipitation collection in the form of rain or dew, while runoff, throughflow, and evapo(transpi)ration contribute to a reduction of water content and a decrease in mass. By monitoring irrigation, runoff, throughflow, and mass changes of the LWS, evapo (transpi)ration and the collection of precipitation can be determined in accordance to:

$$\Delta m_w = \Delta m_{lws} + V_r \rho_w + V_t \rho_w - V_i \rho_w \quad (1)$$

where:

Δm_w = Mass change due to precipitation collection (+) or evapo (transpi)ration (−) [g]
Δm_{lws} = LWS mass change [g]
ρ_w = Density water [g/cm^3]
V_r = Runoff volume [ml]
V_t = Throughflow volume [ml]
V_i = Irrigation volume [ml]

Fig. 5a and b show a simplified representation of the factors influencing the water balance of the panel and the planter box system,

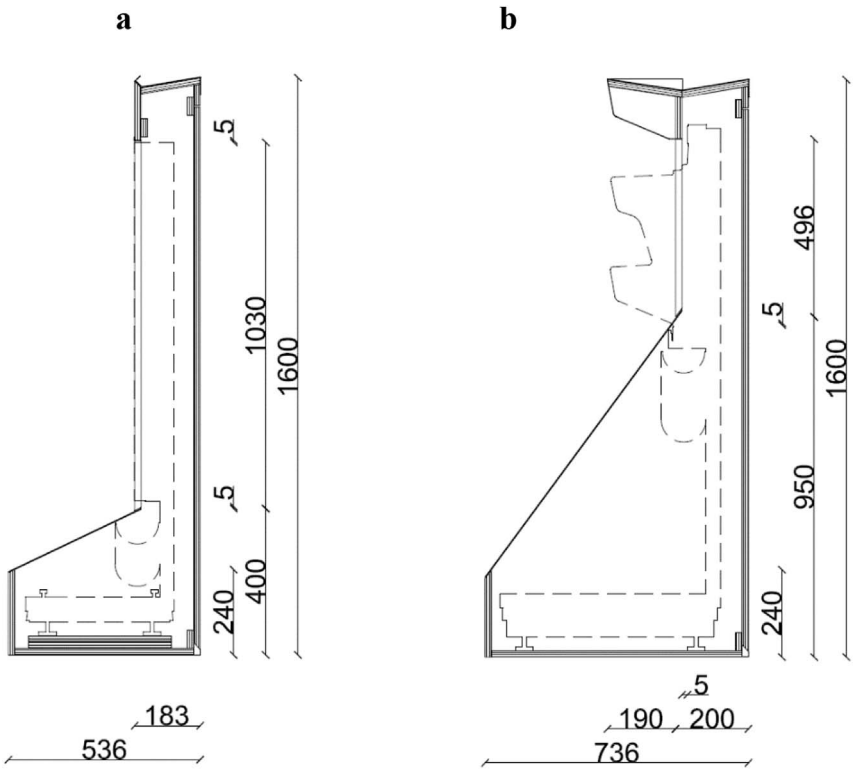

Fig. 4. Cross section of the encasing which houses the planter box systems, balances, mounting stands, irrigation system, and throughflow collection and measurement system (dimensions in mm).

respectively.

2.4. Data acquisition

The mass of the planter box system (including mounting frame ≈33 kg) was monitored directly using a scale with a maximal load of 120 kg and a sensitivity of ± 1 g (Mettler-Toledo, type KC120-ID1 MultiRange). The panel systems mass (including mounting frame ≈25 kg) was directly measured by a scale with a maximum load of 60 kg and a verified sensitivity of ± 10 g in the 15–30 kg range (AllScales Europe, Serie WPI-T-40-60). Both scales were digitally logged continuously up to 6 times per second. A moving average of 22 s was applied to this data to even out wind induced vibrations, yet still show short-term mass variations.

In order to monitor the exact timing and quantity of water added through irrigation, regardless of precipitation or evapo(transpi)ration, an additional external dripper was monitored by a tipping bucket with a calibrated resolution of 0.58 ml/tip. The quantity of water leaving the system in a liquid state (e.g. by running off, or flowing through the system) was determined by collecting effluent water in polytetrafluoroethylene (PTFE) coated gutters and running it directly through tipping buckets.

Fig. 1c depicts the complete test setup with the mounted LWS. Meteorological data is collected continuously during the test period. A Vaisala WTX510 weather station was used to measure barometric pressure, air temperature, relative humidity (RH), wind speed, wind direction, and local precipitation. The weather station is positioned at the same distance from the façade, approximately 0.3 m above the systems, as well as 1.7 m and 3.1 m north of the planter box and the panel system, respectively. Additionally, two rain gauges (Young Model 52202) with a tipping-bucket mechanism and a horizontal orifice were used to measure horizontal rainfall. Their locations on the roof, ± 4 m above the systems, are marked with X in Fig. 1a. The maximum occurring error due to rest water corresponds with the volume of the tipping bucket and the resulting resolution of 0.1 mm of horizontal rainfall per tip. Information on WDR impinging the vertical surface of the façade was determined with a WDR gauge positioned 0.4 m above and in between the two systems. This gauge was designed, manufactured, tested, and optimised in prior studies by the TU/e and has a collection area of 0.2 × 0.2 m with a rest water error corresponding to 0.015 mm [71,72]. The increased accuracy of the WDR gauge over that of the horizontal rain gauges ensures accurate measurements at low catch ratios. Additionally, WDR measurements on the west façade are cross-referenced with those of horizontal rain to eliminate potential false positive readings (e.g. due to condensation). All tipping buckets are regularly checked for proper functioning given the high degree of accuracy and susceptibility to contamination. The occurring hemispherical global solar radiation was determined using a Kipp & Zonen Pyranometer type Solarimeter CM 11 located 1.2 m west of the test setup.

3. Results and discussion

Increases and decreases of the mass of the system are a measure for variations in the water content of the systems. A mass increase represents irrigation, collection of precipitation, or condensation. A decrease in mass can be related to either outgoing streams (runoff and substrate throughflow) or evapo(transpi)ration. Mass variations caused by irrigation, runoff, and throughflow are continuously monitored and their influence corrected for. In turn, this leaves evapo(transpi)ration to be the sole factor for mass loss and precipitation collection and condensation to be the only influencing factors for mass gain.

3.1. Collection of precipitation

Over the test period, 163 precipitation events ranging in magnitude from 0.1 mm to 23.6 mm (Table 1) were measured during 35 of the 61 measurement days. Here, the occurrence of a precipitation event is defined by the detection of rain (no other type of precipitation occurred during the test period) by at least the southern roof mounted rain gauge. Hereby, the influence of the adjacent high rise building on the northern rain gauge and that the façade over the rain gauge close to the

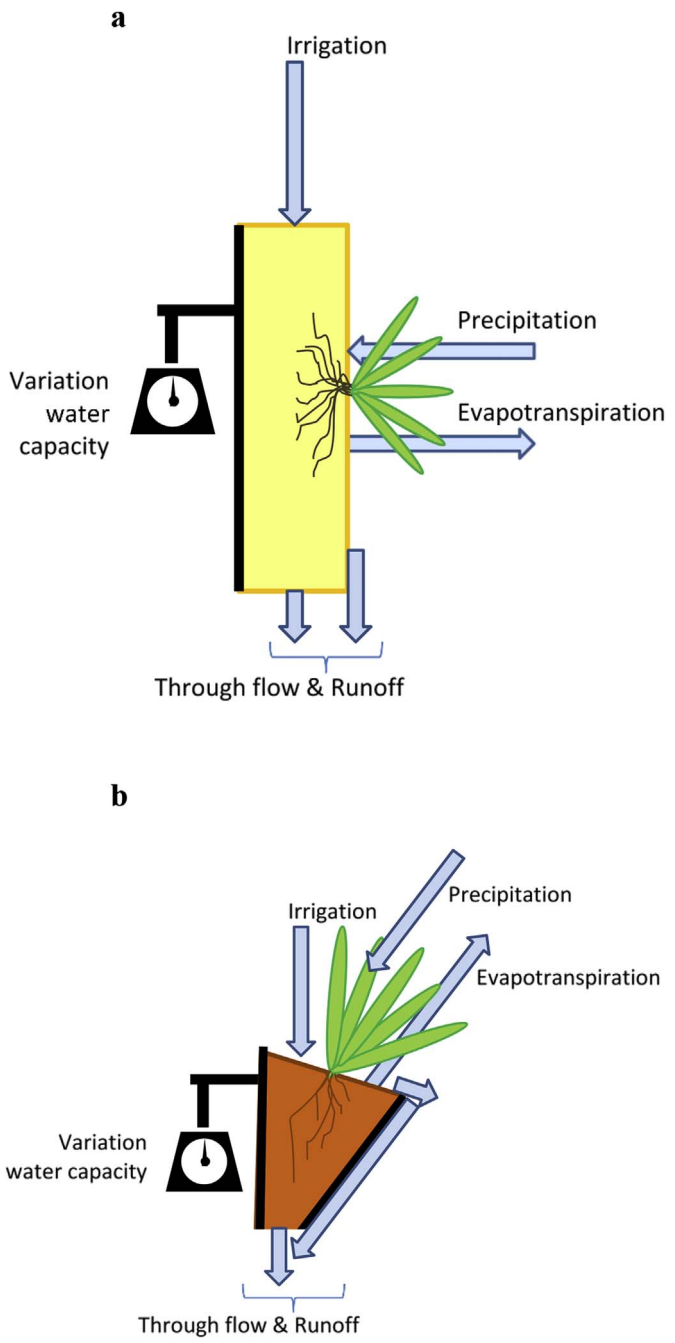

Fig. 5. Schematic representation of influential factors on the water balance of: a. Panel system, b. Planter box system.

systems is avoided. The quantity of collected precipitation was determined by the mass gain determined through Eq. (1). The onset and termination of a precipitation event were cross referenced with the precipitation events detected by the various rain gauges and mass gain through condensation is excluded. Except for 11 events, all being 0.1 mm in magnitude, all precipitation events resulted in a measurable mass change. The precipitation collection of both systems are displayed in Fig. 6a and b for respectively all precipitation events and events smaller than 8 mm. For both systems, a concave trend line can be drawn showing a maximum which can be an indication for the saturation points of the systems, at 1.3 mm and 2.7 mm for respectively the panel system and the planter box system. Since only a limited amount of events larger than 8 mm were recorded and the precipitation collection of these events varies considerably, the exact value of the saturation points is uncertain.

Table 1
Quantity and magnitude of precipitation events measured.

Precipitation magnitude (mm)	Recorded events	Precipitation magnitude (mm)	Recorded events
0.1	62	2.2	2
0.2	20	2.4	2
0.3	10	2.6	1
0.4	11	2.7	1
0.5	6	2.8	3
0.6	5	3.7	1
0.7	3	4.4	1
0.8	4	5.1	1
0.9	10	5.2	1
1.0	2	5.9	1
1.1	1	6.2	1
1.2	2	6.8	1
1.3	1	7.6	1
1.4	2	11.4	1
1.5	1	13.6	1
1.6	1	16.1	1
1.9	1	23.6	1

Both systems vary significantly regarding their substrate. Whereas a volume of ± 67 dm^3/m^2 of mineral wool is applied in the panel system, ± 106 dm^3/m^2 of potting soil is used in the planter box system. In turn, this results in 19 and 25 ml/dm^3 for the panel system and the planter box system, respectively. The composition and hydrodynamic properties of both the mineral wool and the potting soil are unknown and undisclosed by the producers, making reasoning regarding this matter delicate. However, the planter box system was designed with a height of 0.5 m in order to enable capillary rise over its entire height [69] whereas the capillary rise of mineral wool for use in hydroponics is in the region of one order of magnitude lower [73]. This supports the need for the dissimilar approach to irrigation. Through capillary rise, the buffered water in the planter box system is accessible throughout the entire substrate whereby it can used for extended time prior to irrigation. Conversely, the water in the mineral wool of the 1 m high panel system will sag to the lower area, depriving the upper part. Therefore, frequent irrigation is required to ensure enough moisture in the top section, hereby keeping the overall system in a state of high moisture content. These factors combined result in the dissimilarity shown in Fig. 6b.

Expressing the overall precipitation collected on 1 vertical m^2 as an equivalent percentage of the overall precipitation which has fallen on 1 horizontal m^2 results in a global average equivalent percentage of 13.6% and 26.5% for the panel system and the planter box system respectively. However, when the equivalent percentage is calculated for each individual event, the average will be 18.8% for the panel system and 33.0% for the planter box system. The deviation in percentages listed above is an indication that the amount of precipitation captured and retained is reduced with an increase in precipitation intensity. Hence, smaller precipitation events are captured more efficiently than large events. The dissimilarity in precipitation collection between the two systems can be correlated to their designs. The enclosed horizontal surface of the substrate of the planter box is more likely to catch and retain precipitation than the vertical flat substrate provided by the panel system. Additionally, the relatively large volume of potting soil substrate in the planter box system allows for a better and larger buffering capacity, resulting in a less frequently needed irrigation. Hereby, the buffering capacity of the substrate is available and its saturation point is reached less easily and the release of excess water is prevented.

During the test period, the quantity and magnitude of WDR impinging the vertical surface of the west façade were measured with a driving rain gauge. 83 out of 163 occasions WDR was detected. Fig. 7a and b depict the relationship between the collection rate of the panel system and the planter box system respectively and the WDR to

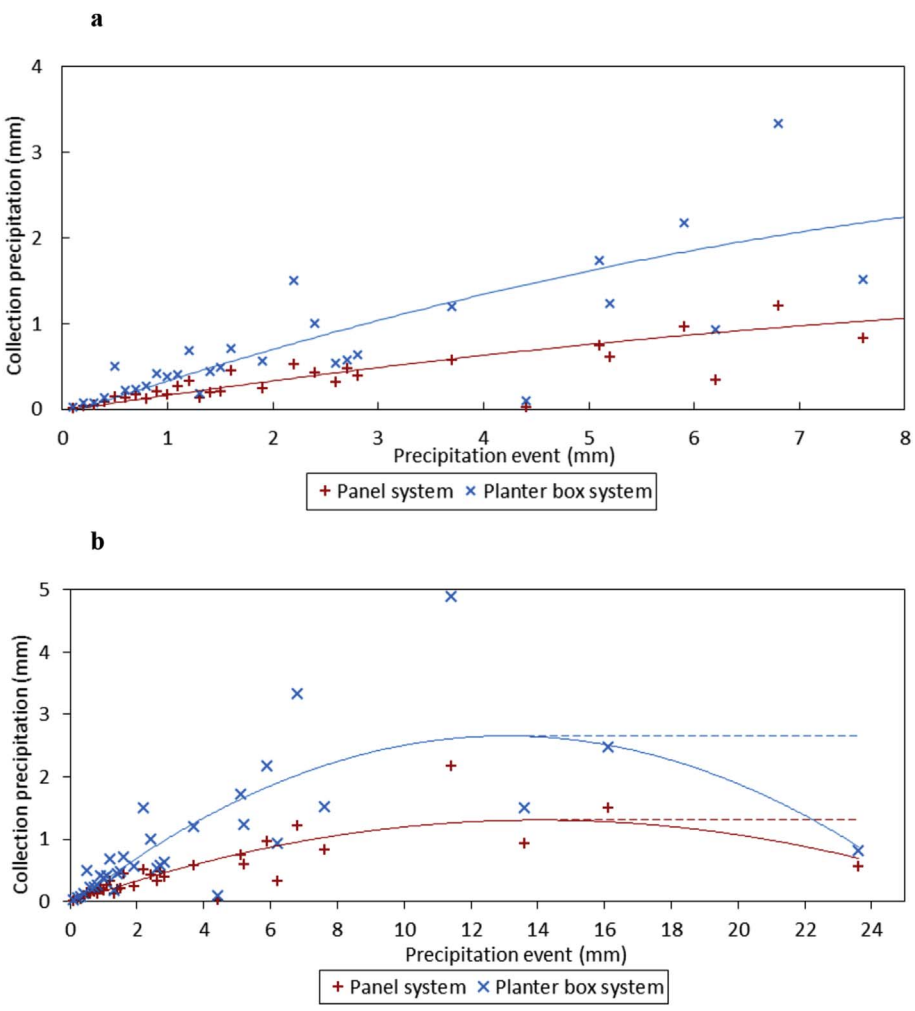

Fig. 6. Precipitation collected (mm) related to the total of the precipitation event (mm) for: a. Events smaller than 8 mm, b. All precipitation events.

horizontal precipitation ratio. As previously mentioned, the average collection rates of both the panel system (18.8%) and planter box system (33.0%) are found to be higher than the 7.7% average WDR.

Of the total of 163 precipitation events, 80 occurred without detection of WDR on the designated gauge. Of these, a mass increase was detected for 63 and 67 of the events for respectively the panel system and the planter box system. Hence, the systems were able to collect precipitation in 78.8% and 83.8% of cases without WDR measured. Potentially, this could be due to low rainfall intensities combined with a higher wind speeds. In this case raindrop diameters and inherent inertia are small which results in a more pronounced distortion in their trajectories [74]. Compared to the WDR rain gauge close to the façade, the plants extruding from the systems have a less pronounced wind blocking effect enabling them to capture droplets with trajectories close to parallel with the façade. The remaining of these precipitation events, which have not led to an increase of weight of the panel system, were all of the smallest precipitation magnitude of 0.1 mm except for one, which was 0.3 mm. This can be attributed to a low horizontal rainfall intensity combined with a low wind speed resulting in a reduced catch ratio or non-west wind directions with limited to absent rain on the test façade [66]. Overall, the planter box system has been found to collect more during events without WDR measured, as well as more WDR than the panel system does. Additionally, it has been found that both systems are able to collect precipitation even if no WDR is measured.

3.2. Evapo(transpi)ration

The analysis of the mass data took place after the measured outflow and the irrigation were calculated for. This left a processed mass graph showing only three streams: collected precipitation, condensation, and evapo(transpi)ration. The limited effect of condensation, being the opposite of evaporation, is effectively cancelling out by deduction. To determine the systems net evapotranspiration (ET) independent of the evaporation due to collected precipitation, both mechanisms of evaporation are processed separately. A typical evapo(transpi)ration prior to and after precipitation is shown in Fig. 8. Excluding condensation and the evaporation related to the collection of precipitation, the remaining total deviation in a systems mass over the considered time period is interpretable as the evapotranspiration of the systems.

By using the latent heat of vaporization of water (2.45 MJ/kg at 20 °C [39]), the weight loss due to evaporation per m^2 façade surface can be converted from mm (l/m^2) into evaporative power (W/m^2). On average, the panel system and the planter box system evapo(transpi) rate respectively 0.75 mm and 0.81 mm per day over the measurement period. The corresponding average evaporative powers (P_{total}) are therefore 21 W/m^2 and 23 W/m^2. Next to the P_{total}, Table 2 also shows the evapotranspirative power (P_{et}) and the evapo(transpi)ration taking place after a precipitation event (P_{evap}). These results show clear differences between the two systems. The panel system evapotranspirates more, thereby evaporating more during dry periods, while the planter box system evaporates more after it has collected precipitation. A possible explanation can be found in the availability of water at a given moment. Since the panel system is irrigated regularly, water is continuously available while the planter box system, due to its design, benefits from the higher degree of precipitation collection.

The planter box system is irrigated more efficiently, needing less

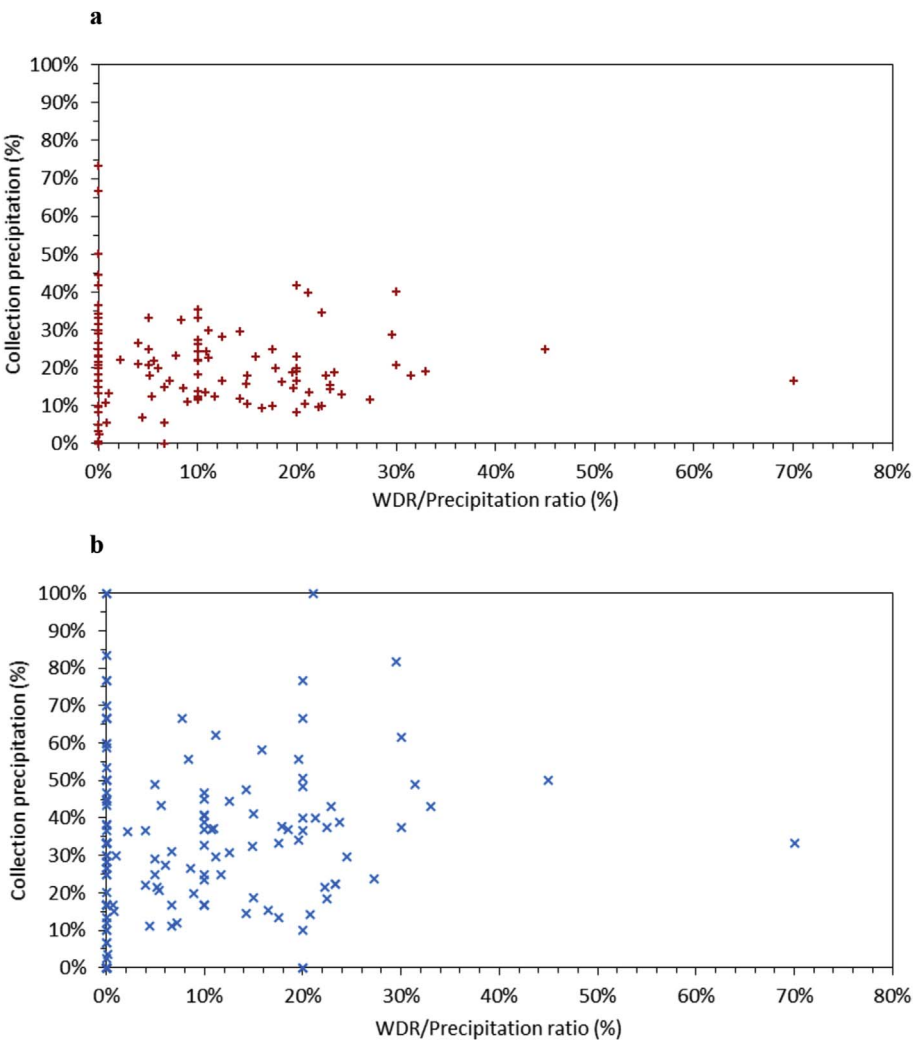

Fig. 7. Percentage of the total precipitation collected relative to the WDR to horizontal precipitation ratio for: a. Panel system, b. Planter box system.

water, yet is dependent on precipitation. For the green façade to function properly all year round, irrigation is to be provided.

3.3. Influencing factors of evapotranspiration

The typically used PM equation specifies how various weather conditions influence the reference evapotranspiration (ET_0), the ET of "a hypothetical reference crop with an assumed crop height of 0.12 m, a fixed surface resistance of 70 s/m, and an albedo of 0.23" which "closely resembles an extensive surface of green grass of uniform height" [39]. For the ET_o, the FAO-56 Penman-Monteith Equation is given as (established in [39]):

$$ET_0 = \frac{0.408\Delta(R_n - G) + \gamma\left(\frac{900}{T+273}\right)u_2(e_s - e_a)}{\Delta + \gamma(1 + 0.34u_2)} \quad (2)$$

where:

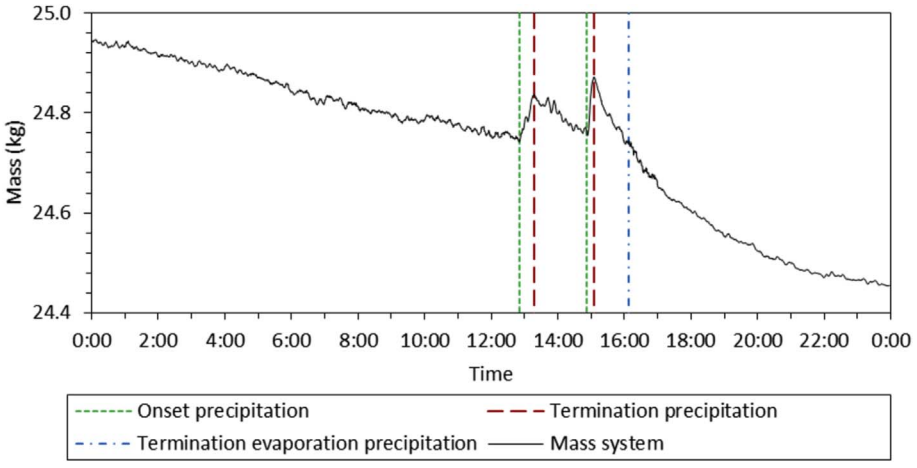

Fig. 8. Typical mass loss and gain due to collection of precipitation, evapotranspiration, and evapo(transpi)ration for the panel system (November 27, 2011).

Table 2
Evapo(transpi)rative power of the panel system and the planter box system: total evaporative power (P_{total}), evapotranspirative power (P_{et}), and precipitation evaporative power (P_{evap}).

		Panel system	Planter box system
P_{et}	(W/m^2)	14.2	9.9
P_{evap}	(W/m^2)	5.5	11.3
P_{total}	(W/m^2)	19.7	21.2

ET_0 = reference evapotranspiration [mm/day],
R_n = net radiation at the crop surface [MJ/m^2/day],
G = soil heat flux density [MJ/m^2/day],
T = mean daily air temperature at 2 m height [°C],
u_2 = wind speed at 2 m height [m/s],
e_s = saturation vapour pressure [kPa],
e_a = actual vapour pressure [kPa],
Δ = slope of the saturated vapour pressure curve [kPa/°C],
γ = psychometric constant [kPa/°C].

In this equation, the soil heat flux density (G) for a vegetation covered surface with calculation time steps of 24 h or longer is relatively small compared to R_n and may be ignored (G ≈ 0) given that the temperature of the substrate follows the air temperature. Furthermore, the saturation vapour pressure deficit is specified through e_s-e_a and the psychometric constant (γ) depends on the atmospheric pressure through [39]:

$$\gamma = \frac{c_p P}{\varepsilon \lambda} = 0.665 \cdot 10^{-3} P \tag{3}$$

$$P = 101.3\left(\frac{293 - 0.0065z}{293}\right)^{5.26} \tag{4}$$

were:

λ = latent heat of vaporization, 2.45 [MJ/kg],
c_p = specific heat at constant pressure, 1.013 10^{-3} [MJ/kg/°C],
ε = molecular mass ratio of water vapour and dry air, 0.622 [-],
z = elevation above sea level [m].
P = atmospheric pressure [kPa],
Δ, the slope of the saturated vapour pressure curve, is the derivative of the saturated vapour pressure e°(T), and therefore determined by the air temperature through the following equations [39]:

$$e^{\circ}(T) = 0.6108 e^{\left(\frac{17.27T}{T+237.3}\right)} \tag{5}$$

$$\Delta = \frac{4098 e^{\circ}(T)}{(T + 237.3)^2} \tag{6}$$

were:

e°(T) = saturation vapour pressure at the air temperature T [kPa],
T = mean daily air temperature at 2 m height [°C].

Hence, the influential climatological parameters determining ET_0 are wind speed, saturation vapour pressure deficit (humidity), air temperature, and solar radiation. The test setup is located 27.5 m above sea level (ground level location, 16.0 m [75]; balcony, 10.4 m; average mounting height 1.1 m), resulting in a psychometric constant (γ) of 0.067 kPa/°C. Substituting the constant values (G and γ) into Eq. (2), gives the following:

$$ET_0 = \frac{0.408\Delta R_n + \left(\frac{60.3}{T+273}\right) u_2 (e_s - e_a)}{\Delta + 0.023 u_2 + 0.067} \tag{7}$$

For the start, middle, and end of the test period (respectively November 24, December 26, and January 29), the ET_o is determined based on the long-term average meteorological conditions for Eindhoven given in Table 3 [68]. Fig. 9a displays the influence of wind speed on the ET_o. As can be seen, the graphs show a curvature which is best captured by a polynomial equation. In the measured wind speed range of 0.3 m/s to 4.6 m/s, however, the correlations shown in Fig. 9a are close to linear with an R^2 value of 0.98. Hence, to avoid the influence of scattering due to other influential factors, it is chosen to display the trend between measured ET and wind speed linearly (Fig. 9b).

Table 3
Long-term average meteorological conditions for Eindhoven, the Netherlands [68].

		Nov	Dec	Jan
T_{min}	(°C)	3.3	0.8	0
T_{max}	(°C)	9.6	6.1	5.7
u_z	(m/s)	4.1	4.4	4.9
z	(m)	10	10	10
Rh_{mean}	(%)	76	86	87

The saturation vapour pressure deficit of the air, being the difference between saturation vapour pressure and actual vapour pressure, is a measure of the capacity of air to take up water vapour before being saturated. During the test, temperature and relative humidity are monitored, enabling the calculation of saturation vapour pressure deficit through [39]:

$$e_s = \frac{e^{\circ}(T_{max}) + e^{\circ}(T_{min})}{2} \tag{8}$$

$$e_a = \frac{e^{\circ}(T_{max})\frac{RH_{max}}{100} + e^{\circ}(T_{min})\frac{RH_{max}}{100}}{2} \tag{9}$$

where.

$e^{\circ}(T_{min})$ = saturation vapour pressure at daily minimum temperature [kPa],
$e^{\circ}(T_{max})$ = saturation vapour pressure at daily maximum temperature [kPa],
T_{max} = daily maximum air temperature at 2 m height [°C],
T_{min} = daily minimum air temperature at 2 m height [°C],
RH_{max} = maximum relative humidity [%],
RH_{min} = minimum relative humidity [%].

Based on the meteorological data given in Table 3 [68], the ET_o is calculated for a range in the vapour pressure deficit (Fig. 10a). As could be concluded from Eqs. (2), (8) and (9), the variation in ET_o is linear. Fig. 10b shows the determined saturation vapour pressure deficit related to the measured ET. Here, despite a scattering due to other influencing factors, a linear correlation can be seen.

As seen in Eq. (2), the air temperature is directly present in the PM equation, in the mean saturated vapour pressure (e_s; Eq. (8)), as its derivative, the slope of the saturated vapour pressure curve (Δ; Eq. (6)), and in the actual vapour pressure (e_a; Eq. (9)). Fig. 11a displays the ET_o based on Table 3 [68] for a broad air temperature range. During the test period, temperatures between 0 °C and 8 °C were detected for which the graph can be perceived as linear. However, due to the slope of the saturated vapour pressure curve (Δ; Eq. (6)), a second-degree polynomial correlation between ET_o and temperature exists. Furthermore, as for wind speed, with an R^2 value of 1.00, the correlation displayed in Fig. 11a is near linear. Since the temperature variable is present in correlation with all other influential factors, a larger scatter is to be expected for the correlation between temperature and ET, so the trend lines in Fig. 11b are presented linearly.

To determine the relation between evapotranspiration and incident radiation (R_n) and to exclude the effect of evaporation of precipitation, only the daily global radiation period (8:00–17:00) of the 18 and 23 successfully measured dry days for respectively the panel and the

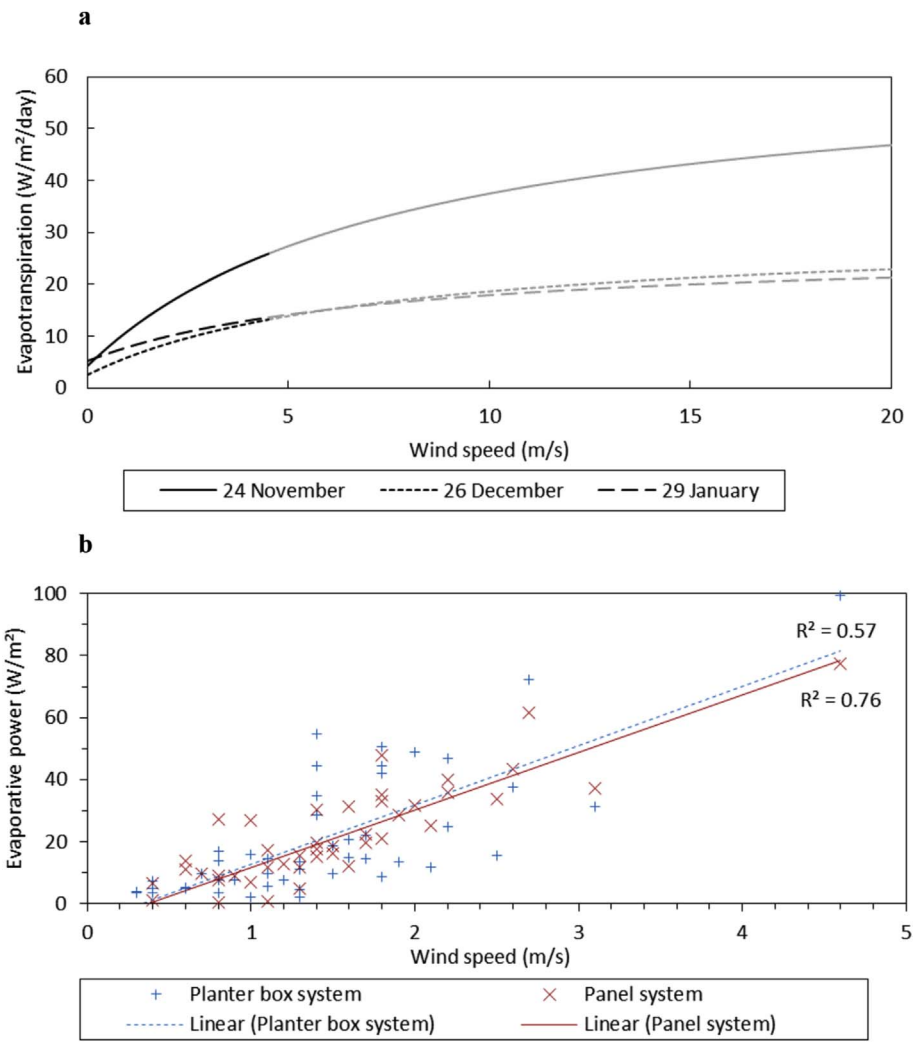

Fig. 9. Evapotranspiration related to wind speed for: a. Theoretical ET_o based on average meteorological conditions at the start, middle, and end date (measurement range in black); b. Measured ET.

planter box system, was used for analysis. Fig. 12a shows the radiation curve and corresponding ET curve of the planter box system for November 19, 2011. Fig. 12b displays the radiation plotted against the ET showing a linear correlation. Once more, deviations from the linear correlation occur due to variations in the other influential factors (e.g. wind speed, water vapour content of the air, and temperature) over the radiation period. In both graphs, the influence of the west orientation of the systems ET and incident radiation can clearly be seen. The range and mean evaporative power and the corresponding percentage of incoming radiation used for ET of all prior mentioned events are given in Table 4. These percentages are in range with the 20%–40% of ET from radiation, found by Krusche et al. for plants on the open ground [24]. The evaporative power by radiation is in the same range as the values presented in Table 2. The variation can be explained by the ET taking place outside of radiation hours, which is taken into account for the values in Table 2, as well as the increased amount of evaporation occurring on days with precipitation.

The analysis of the influencing factors has shown that none are independent, yet the trend lines for both the panel and the planter box system are in good correlation. Hence, based on the determined weather conditions, the ET_o is calculated for each measurement day. Fig. 13a and b display the correlation between the calculated and the measured evaporation for the panel system and the planter box system respectively. As witnessed with the individual climatological factors, the ET of the panel system shows a more narrow spread and, therefore, a better correlation than the planter box system.

3.4. Evapotranspiration prognosis

The effect of characteristics distinguishing a crop from the hypothetical reference crop is integrated into a crop coefficient (K_c). Furthermore, a water stress coefficient (K_s) is used to describe soil water stress effects. Herewith, the crop evapotranspiration under standard conditions (ET_c) and the crop evapotranspiration adjusted for stress conditions ($ET_{c\ adj}$) are given by [39]:

$$ET_c = K_c ET_o \tag{10}$$

where:

ET_c = crop evapotranspiration under standard conditions [mm/day]
K_c = crop coefficient [-]

In contrast to the horizontal square meter of the reference crop, the considered surface is a west-oriented vertical square meter. Being either ascending or descending, without additional support, the growth direction of plants is vertical. Hence, the thickness of the foliage on a vertical surface is more limited than the height of vegetation on a horizontal surface. Furthermore, the structure to the east side of the vegetation casts a shadow over the vegetation for half of the day, a situation which is comparable to the presence of tall border vegetation. Both this and the crop height can be taken into account in the PM equation by the adjustment of the K_c value.

Compared to the reference, a relatively small volume of substrate

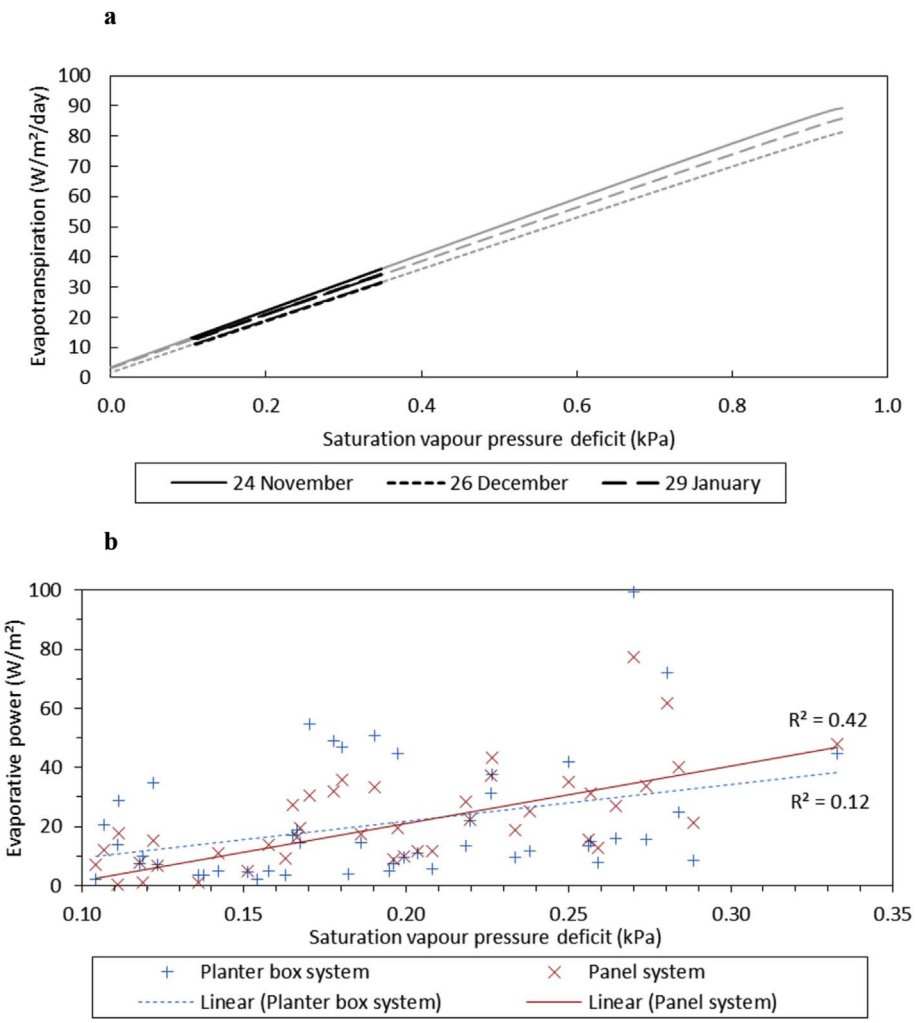

Fig. 10. Evapotranspiration related to saturation vapour pressure deficit for: a. Theoretical ET_o based on average meteorological conditions at the start, middle, and end date (measurement range in black); b. Measured ET.

without underlying water buffer is available. To overcome this dissimilarity, the condition of the well-watered soil is provided by properly irrigating the systems through which actual water stress is prevented.

On both systems, the vegetation was selected for both their compatibility with the system and to obtain a representative value for the diverse foliage applied in a practical situation. This situation is consistent with the intercropping described in the PM equation for which the K_c value can be altered to achieve a mean value for multiple crops.

All previously described deviations show to have a similar effect, which can be accounted for by altering the K_c value. Consequently, it is assumed that a coefficient can be used to incorporate the effect of the before mentioned characteristics which distinguish the tested LWS from the hypothetical reference crop. The implementation of this factor, K_{LWS}, results in the following equation:

$$ET_{LWS} = K_{LWS} ET_o \quad (11)$$

where:

ET_{LWS} = living wall system evapotranspiration under standard conditions [mm/day]
K_{LWS} = living wall system coefficient [-]

Based on the theoretical ET_o, calculated with the measured daily mean weather data, and observed ET (Fig. 13a and b), a value for the correlation is determined. For the panel and the planter box system, this results in average K_{LWS} coefficients of approximately 1.46 and 0.76, respectively. Fig. 13a and b show that the correlation for the panel system (R^2 = 0.70) is better than that of the planter box system (R^2 = 0.28). Hence, the standard error (dashed lines in Fig. 13a and b) is taken into account for the determination of the year-round ET_{LWS} using the K_{LWS} values.

The value for the planter box system is in the range of that of onion and sorghum at the end of the season (K_c = 0.75) [76,77]. Based on a review article by Lazzara and Rana [78,79] reporting K_c values ranging from 0.1 to 1.78, the value determined for the panel system is relatively high, only exceeded by alfalfa in the middle of the season (1.78), with a value close to that of green beans (Helda) in the middle of the season in a greenhouse (K_c = 1.4) [80]. With K_{LWS} coefficients of 1.46 and 0.76, there is a 70% difference between the panel and the planter box system. This can be related to the abundance of water in the panel system in combination with the dissimilarity in the designs. While the exterior encasing of the planter box system is made of watertight plastic, leaving only a small substrate surface exposed, the panel systems exterior consists of a geotextile with a large surface which enables additional evaporation. This effect correlates with soil evaporation which occurs when a crop is small and hardly covers the ground. Hence, due to the high frequency of irrigation, the effect of evaporation will be considerable, whereby K_c may exceed unity [39]. The year-round reference crop ET_o is calculated by implementing standard local climatological records of wind speed, humidity, air temperature, and solar radiation into the PM equation (Eq. (2)). Fig. 14 shows the ET_o and the ET_{LWS} obtained through the application of the K_{LWS} coefficients for both systems. Based on these prognoses, the ET of the panel system results in 650 (± 100) mm/year and the ET of the planter box system in 380

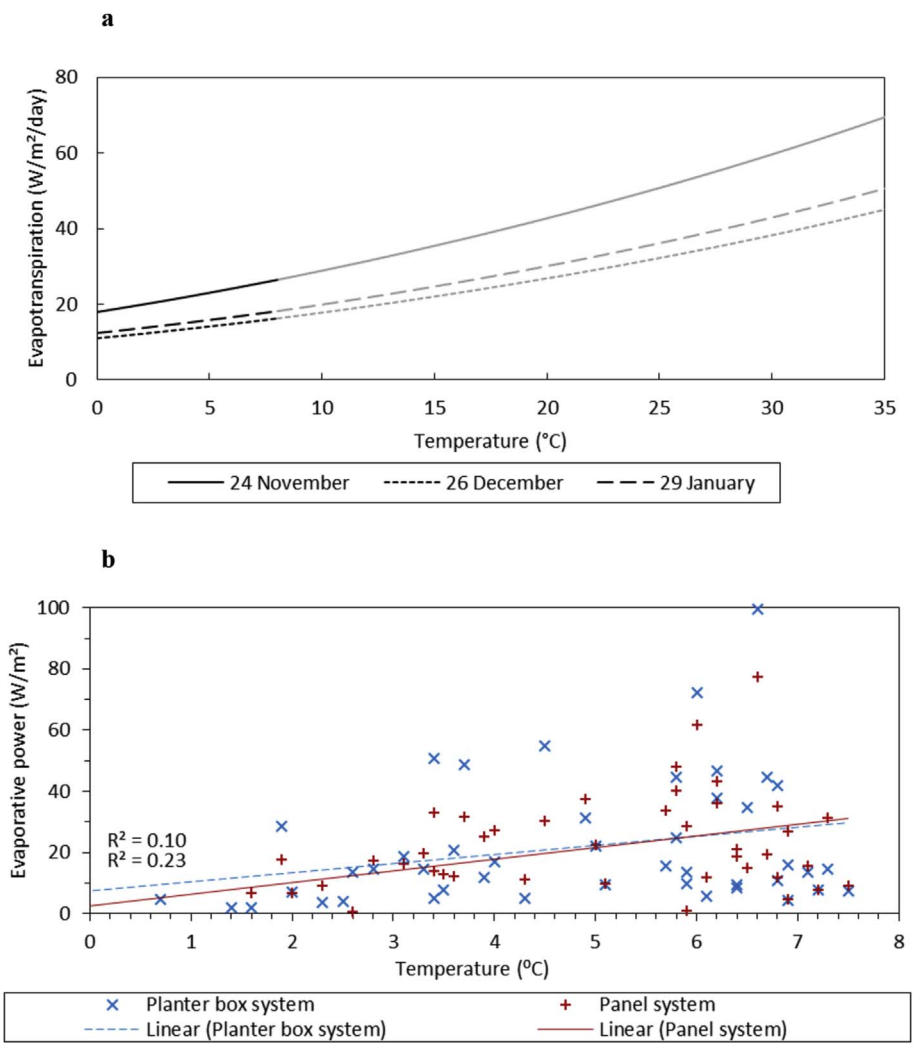

Fig. 11. Evapotranspiration related to temperature for: a. Theoretical ET_o based on average meteorological conditions at the start, middle, and end date (measurement range in black); b. Measured ET.

(± 120) mm/year, hence translating to respectively 18 (± 3) kW/m^2/year and 11 (± 3) kW/m^2/year, reaching a peak of 83 (± 12) W/m^2/day and 47 (± 12) W/m^2/day.

3.5. Water balance systems

With the obtained data, the magnitude of all in- and outgoing water streams is established for both systems on a daily basis. This results in the average water balances for the overall test period. Fig. 15a and b show the water balance where the entering amount of water is set to be 100%. Fig. 15c and d show the balances when the total average precipitation of 3.36 mm per horizontal m^2 per day is set as 100%. Since this amount is equal for both systems, quantities can be compared directly. The larger amount of applied irrigation to the panel system can be clearly distinguished as a major influence on the overall entering amount of water. With a total inflow of 2.12 mm/day, the planter box system takes in more than double the amount of water it processes with 0.99 mm/day. With an average combined runoff and throughflow of 1.31 mm/day and an increase 0.06 mm/day in the buffer, the planter box system is found to receive an excess of irrigation. A reduction of the irrigation with 1.37 mm/day, however, would be inadequate, since part of the runoff and throughflow measured is related to the runoff during and after precipitation. In turn, this correlates with the design of the panel system of a vertical semi-penetrable surface and a mineral wool substrate with a reduced buffer capacity. With an overall 0.03 mm/day decrease in the internal buffer of the planter box system, increasing the frequency of irrigation is suggested, however, the runoff and throughflow are on average larger. During the summer period, the calculated ET of the panel and the planter box system is approximately 3.6 times higher than that of the test period. Considering this, the irrigation for both systems during this period should be increased to maintain a situation where water stress is avoided. When this condition is met, the ET is independent of the magnitude of the incoming water flows, provided that they are larger than the calculated ET. As mentioned earlier, the ET of both systems, including the ET of precipitation, is almost equal for both the panel system and planter box system. This, being higher than the evapotranspiration determined for the dry periods, indicates that the actual energy absorbed and used for evaporation is higher than calculated. Yet, more research over a longer time span is needed to give an indication of this value. The values of ET determined in this study are plausible given the prior research on the ET of Parthenocissus tricuspidata, Hedera helix, and Fallopia baldschuanica covered façades in Berlin, Germany, respectively showing a daily evaporation of 0.7–1.3 l/d/m^2, 1.2–1.7 l/d/m^2, 0.7–2.3 l/d/m^2 façade area in August and October [81].

4. Conclusion and recommendations

Two living wall systems, a panel system and a planter box system, were tested over a period of 2 months under outdoor conditions. During this period, all administered incoming and outgoing streams of water were monitored as well as all occurring weather conditions (e.g. irradiation, precipitation, wind, wind driven rain, relative humidity, etc.). The mass of both systems was monitored continuously to determine

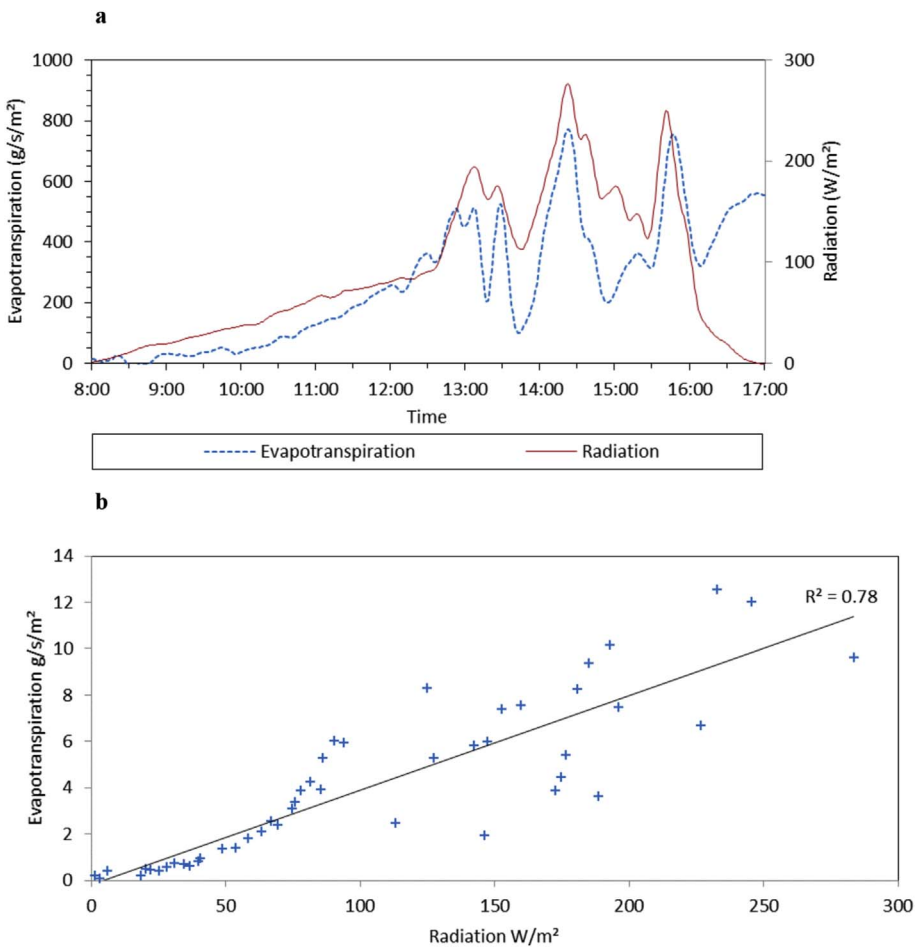

Fig. 12. Solar radiation and evaporation correlation of the planter box system (November 19, 2011) for: a. Time dependent correlation; b. Time independent correlation.

Table 4
Minimum, maximum and mean evapo(transpi)rative power (P_{min}, P_{max}, and P_{mean} respectively) and minimum, maximum and mean percentage of incident solar radiation used for evapotranspiration ($R_{n\ min}$, $R_{n\ max}$, and $R_{n\ mean}$ respectively) by the panel system and the planter box system.

ET		Panel system	Planter box system
$P_{et\ min}$	(W/m^2)	3	5
$P_{et\ max}$	(W/m^2)	31	40
$P_{et\ mean}$	(W/m^2)	16.1	19.0
$R_{n\ min}$	(%)	4	16
$R_{n\ max}$	(%)	38	36
$R_{n\ mean}$	(%)	19.6	24.0

changes to the internal water content due to precipitation, condensation, and evapo(transpi)ration. The resulting water balances distinguish and quantify the entering liquid water; by irrigation, precipitation and condensation, outgoing liquid water; by means of runoff & throughflow, and outgoing gaseous water through evapo(transpi)ration. It is shown that the tested living wall systems are able to collect precipitation as well as, to varying degrees, buffer it for later evapo(transpi)ration.

Precipitation events ranging from 0.1 mm to 23.6 mm were collected and absorbed by the panel as well as the planter box system. For both systems, the buffering capacity has been found to be exceeded with precipitation events larger than approximately 13 mm. Hence, the buffering capacity is used most efficiently during smaller precipitation events. The systems do not have to face the wind, nor does the precipitation have to occur at an angle to the systems for collection to take place. However, the planter box system shows to collect more precipitation under the influence of wind driven rain than the panel system with a collection rate of respectively 26.5% and 13.6% of the total precipitation that falls on a horizontal m^2. Here, the horizontal surfaces of the planter box system enable it to catch and absorb the precipitation more easily. In addition to that, this system contains a substrate with a high buffering capacity, as a result of which it needs little irrigation during a rainy period.

The collection of precipitation contributes to evapo(transpi)ration. Hereto, the panel and the planter box system utilise respectively 4%–38% and 16%–36% of the incident solar radiation. On average, an evaporative power of 21 W/m^2 for the panel system, and 23 W/m^2 for the planter box system have been achieved during the test period. Next to the mild insulating effect and the shadow provided by a green façade, evapo(transpi)ration can be considered as an additional passive cooling mechanism which becomes active when solar radiation increases, so when cooling is actually desired.

The application of the FAO Penman-Monteith model indicates a higher potential for evaporation for the panel system compared to the planter box system. The expected energy uptake and associated cooling potential of the panel and planter box system are 18 (± 3) kW/m^2/year and 11 (± 3) kW/m^2/year, respectively, reaching a peak at 47 (± 12) W/m^2/day and 83 (± 12) W/m^2/day. Hence, the exposed surface combined with the regular irrigation on daily basis, ensuring a continuous highly humid substrate of the panel system, strongly influenced the evapo(transpi)ration of the panel system and should therefore not be neglected. To support the calculated rate of evaporation during summer, the planter box system, like the panel system, needs a higher degree of irrigation than provided during the test period.

To gain more knowledge on the subject, this study can be prolonged by year-round testing of the selected systems. This will provide more data on both the collection of precipitation and the evaporative performance under a more diverse variety of weather conditions. In

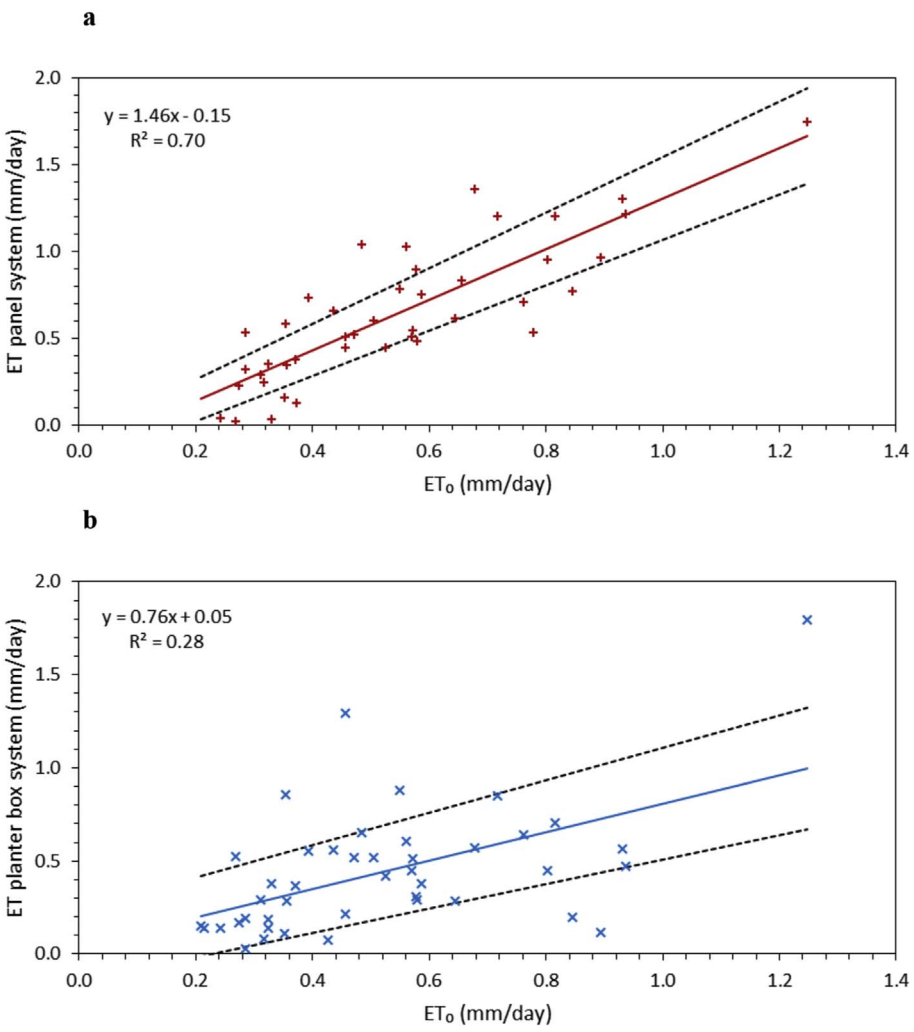

Fig. 13. Measured evaporation related to the calculated ET_o based on occurring weather conditions, dotted lines indicate the standard error for: a. Panel system; b. Planter box system.

addition, a comparative study into precipitation collection and evaporative cooling of a wider range of façade greening systems and commonly applied façade materials can be performed. Hereby, the added value of different approaches, continuous irrigation and the active role of vegetation contributing to the ET, can be determined. Moreover, since the available surface of a green façade (e.g. layers of leaves and flowers) is larger than that of common façades, the combination of collection and buffering of precipitation prior to evapo(transpi)ration is more likely. Besides expanding the study in a temperate maritime climate, the precipitation collection and ET could be investigated in a different climate, e.g. a hot and dry climate, where humidity is low and cooling is needed, or a warm and humid climate, where thermal comfort is an issue and vegetation will thrive. Furthermore, all of the proposed case studies can help to improve the calculated evaporation prognosis based on the Penman-Monteith model.

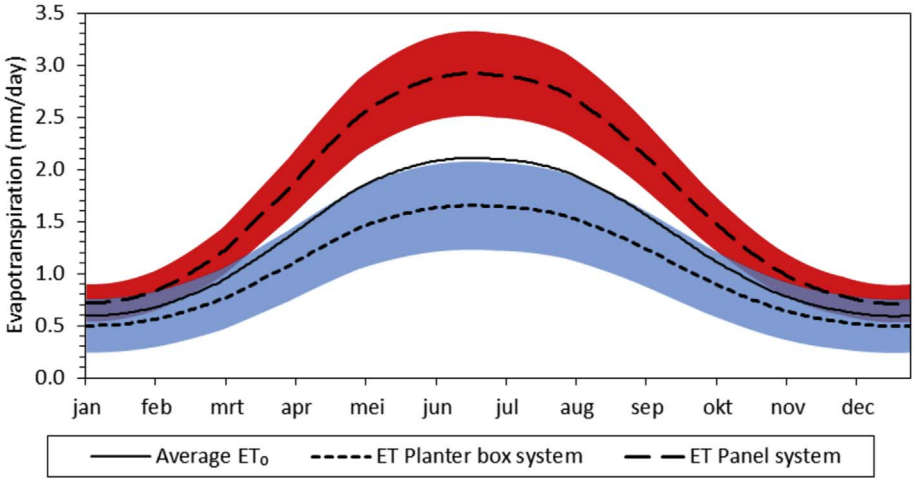

Fig. 14. Calculated average open ground evapotranspiration Eindhoven and prognosis for the evapotranspiration of the panel and the planter box system throughout the year (standard error range indicated), by means of the FAO Penman-Monteith model.

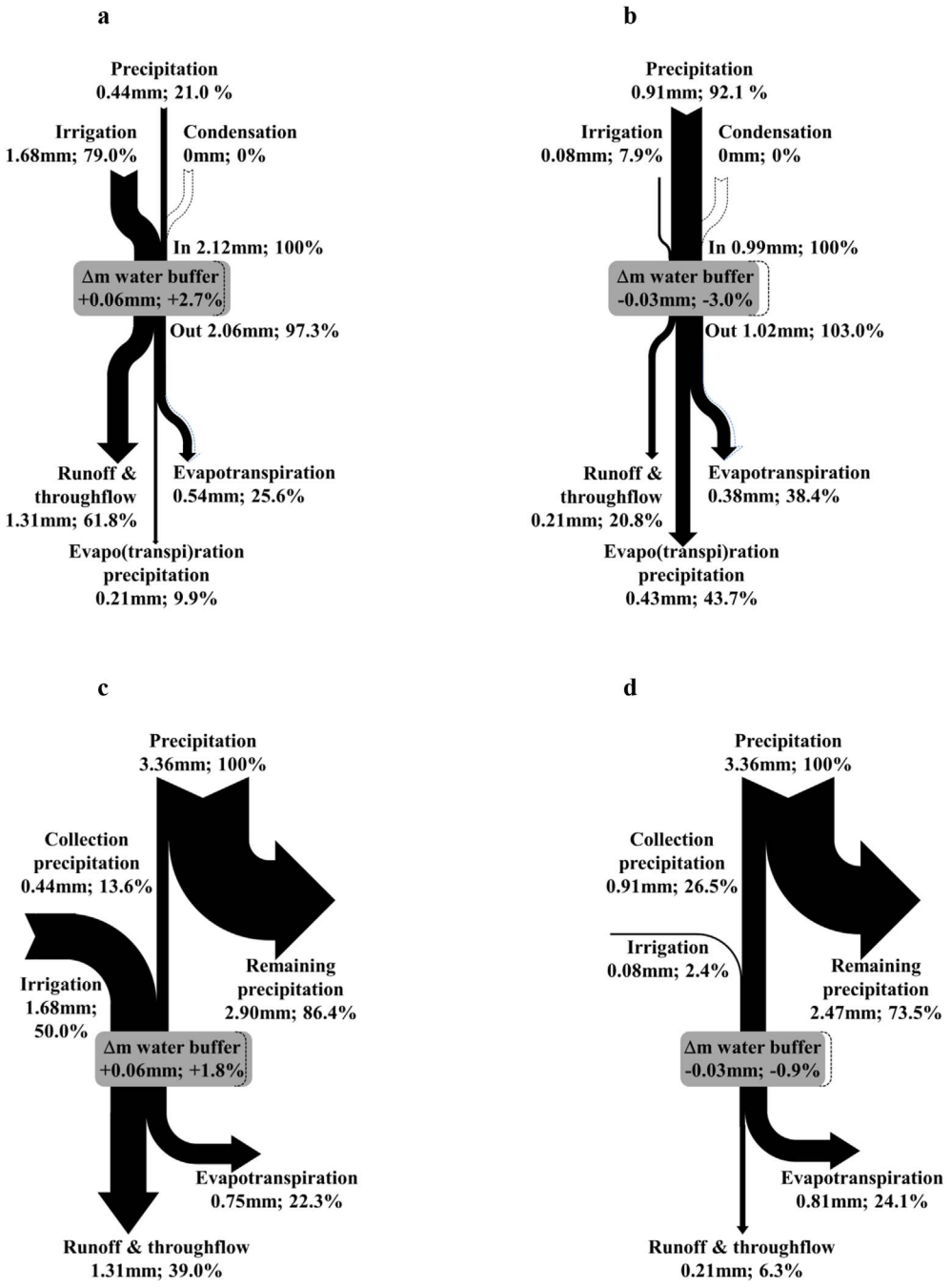

Fig. 15. Water balances where condensation (dotted) is taken into account as negative evapotranspiration: a. Water balance panel system in total, incoming flows set to 100%; b. Water balance planter box system in total, incoming flows set to I00%; c. Water balance panel system related to precipitation; d. Water balance planter box system related to precipitation.

Acknowledgements

The authors wish to express their gratitude to Greenwave Systems for supplying the planter box system and Wallflore® for their provision of the PER-e panel system, as well as to the Cement-Concrete-Immobilisates sponsor group at TU Eindhoven: Rijkswaterstaat Grote Projecten en Onderhoud, Graniet-Import Benelux, Kijlstra Betonmortel, Struyk Verwo, Attero, Enci, Rijkswaterstaat Zee en Delta - District Noord, Van Gansewinkel Minerals, BTE, V.d. Bosch Beton, Selor, GMB, Icopal, BN International, Eltomation, Knauf Gips, Hess AAC Systems, Kronos, Joma, CRH Europe Sustainable Concrete Centre, Cement & BetonCentrum, Heros, Inashco, Keim, Sirius International, Boskalis, NNERGY (chronological order of joining).

References

[1] B.C. Wolverton, Foliage plants for improving indoor air quality, Natl. Foliage Found. Inter. Semin, 1988 Hollywood, FL; United States https://ntrs.nasa.gov/search.jsp?R=19930073015.
[2] M. Ottelé, Vertical Greened Surfaces and the Potential to Reduce Air Pollution and the Improvement of the Insulation Value of Buildings, (2010) http://edepot.wur.nl/139009.
[3] J. Mentens, D. Raes, M. Hermy, Green roofs as a tool for solving the rainwater runoff problem in the urbanized 21st century? Landsc. Urban Plan. 77 (2006) 217–226, http://dx.doi.org/10.1016/j.landurbplan.2005.02.010.
[4] H.S. Yang, J. Kang, M.S. Choi, Acoustic effects of green roof systems on a low-profiled structure at street level, Build. Environ. 50 (2012) 44–55, http://dx.doi.org/10.1016/j.buildenv.2011.10.004.
[5] M.R. Ismail, Quiet environment: acoustics of vertical green wall systems of the Islamic urban form, Front. Archit. Res. 2 (2013) 162–177, http://dx.doi.org/10.1016/j.foar.2013.02.002.
[6] J. Kang, M. Zhang, Semantic differential analysis of the soundscape in urban open public spaces, Build. Environ. 45 (2010) 150–157, http://dx.doi.org/10.1016/j.buildenv.2009.05.014.

[7] T. Van Renterghem, D. Botteldooren, Numerical evaluation of sound propagating over green roofs, J. Sound. Vib. 317 (2008) 781–799, http://dx.doi.org/10.1016/j.jsv.2008.03.025.
[8] R.S. Ulrich, R.F. Simons, B.D. Losito, E. Fiorito, M.A. Miles, M. Zelson, Stress recovery during exposure to natural and urban environments, J. Environ. Psychol. 11 (1991) 201–230, http://dx.doi.org/10.1016/S0272-4944(05)80184-7.
[9] V.I. Lohr, C.H. Pearsons-Mims, G.K. Goodwin, Interior plants may improve worker productivity and reduce stress in a windowless environment, J. Environ. Hortic. 14 (1996) 97–100 http://www.hriresearch.org/docs/publications/JEH/JEH_1996/JEH_1996_14_2/JEH 14-2-97-100.pdf.
[10] T. Van Renterghem, D. Botteldooren, Reducing the acoustical façade load from road traffic with green roofs, Build. Environ. 44 (2009) 1081–1087, http://dx.doi.org/10.1016/j.buildenv.2008.07.013.
[11] T. Safikhani, A.M. Abdullah, D.R. Ossen, M. Baharvand, A review of energy characteristic of vertical greenery systems, Renew. Sustain, Energy Rev. 40 (2014) 450–462, http://dx.doi.org/10.1016/j.rser.2014.07.166.
[12] E. Schroll, J. Lambrinos, T. Righetti, D. Sandrock, The role of vegetation in regulating stormwater runoff from green roofs in a winter rainfall climate, Ecol. Eng. 37 (2011) 595–600, http://dx.doi.org/10.1016/j.ecoleng.2010.12.020.
[13] K.L. Getter, D.B. Rowe, J.A. Andresen, Quantifying the effect of slope on extensive green roof stormwater retention, Ecol. Eng. 31 (2007) 225–231, http://dx.doi.org/10.1016/j.ecoleng.2007.06.004.
[14] N.D. VanWoert, D.B. Rowe, J.A. Andresen, C.L. Rugh, R.T. Fernandez, L. Xiao, Green roof stormwater retention, J. Environ. Qual. 34 (2005) 1036, http://dx.doi.org/10.2134/jeq2004.0364.
[15] M. Köhler, Green facades-a view back and some visions, Urban Ecosyst. 11 (2008) 423–436, http://dx.doi.org/10.1007/s11252-008-0063-x.
[16] Berlin Senate for Urban Development Communications in Cooperation with Technical University Berlin & University of Applied Sciences Neubrandenburg, Rainwater Management Concepts, Greening Buildings, Cooling Buildings, Berlin Senate for Urban Development, (2010) Berlin, Germany http://www.gruendach-mv.de/SenStadt_Regenwasser_engl_bfrei_final.pdf.
[17] M. Schmidt, The evapotranspiration of greened roofs and façades, Green. Rooftops Sustain. Communities, vol. 2006, Green Roofs for Healthy Cities, Boston, MA, May 11-12, 2006, p. 10.
[18] J. Czemiel Berndtsson, Green roof performance towards management of runoff water quantity and quality: a review, Ecol. Eng. 36 (2010) 351–360, http://dx.doi.org/10.1016/j.ecoleng.2009.12.014.
[19] E.L. Villarreal, L. Bengtsson, Response of a Sedum green-roof to individual rain events, Ecol. Eng. 25 (2005) 1–7, http://dx.doi.org/10.1016/j.ecoleng.2004.11.008.
[20] C. Schade, Wasserrückhaltung und Abflussbeiwerte bei dünnschichtigen extensivbegrünungen, Stadt Und Grün 49 (2000) 95–100.
[21] H.J. Liesecke, Das Retentionsvermögen von Dachbegrünungen, Stadt Und Grün 47 (1998) 437–443.
[22] A. Eggenberger, Bauphysikalische Vorgänge im begrünten Warmdach, Das. Gartenamt 6 (1983).
[23] B. Bass, K.K.Y. Liu, B.A. Baskaran, Evaluating Rooftop and Vertical Gardens as an Adaptation Strategy for Urban Areas, (2003) http://doi.org/10.4224/20386110.
[24] P. Krusche, M. Krusche, D. Althaus, I. Gabriel, Ökologisches Bauen – Herausgegeben vom Umweltbundesamt, Bauverlag GmbH, Wiesbaden & Berlin, 1982 ISBN-10: 3528016752, ISBN-13: 978–3528016753.
[25] A. Hoyano, Climatological uses of plants for solar control and the effects on the thermal environment of a building, Energy Build. 11 (1988) 181–199, http://dx.doi.org/10.1016/0378-7788(88)90035-7.
[26] N.H. Wong, A.Y.K. Tan, P.Y. Tan, N.C. Wong, Energy simulation of vertical greenery systems, Energy Build. 41 (2009) 1401–1408, http://dx.doi.org/10.1016/j.enbuild.2009.08.010.
[27] E.A. Eumorfopoulou, K.J. Kontoleon, Experimental approach to the contribution of plant-covered walls to the thermal behaviour of building envelopes, Build. Environ. 44 (2009) 1024–1038, http://dx.doi.org/10.1016/j.buildenv.2008.07.004.
[28] K.J. Kontoleon, E.A. Eumorfopoulou, The effect of the orientation and proportion of a plant-covered wall layer on the thermal performance of a building zone, Build. Environ. 45 (2010) 1287–1303, http://dx.doi.org/10.1016/j.buildenv.2009.11.013.
[29] P. Sunakorn, C. Yimprayoon, Thermal performance of biofacade with natural ventilation in the tropical climate, Procedia Eng. 21 (2011) 34–41, http://dx.doi.org/10.1016/j.proeng.2011.11.1984.
[30] S. Charoenkit, S. Yiemwattana, Living walls and their contribution to improved thermal comfort and carbon emission reduction: a review, Build. Environ. 105 (2016) 82–94, http://dx.doi.org/10.1016/j.buildenv.2016.05.031.
[31] S.W. Peck, C. Callaghan, Greenbacks from Green Roofs Forging a New Industry in Canada - Status Report on Benefits, Barriers and Opportunities for Green Roof and Vertical Garden Technology Diffusion, (1999) https://www.nps.gov/tps/sustainability/greendocs/peck-sm.pdf.
[32] G.S. Campbell, J.M. Norman, An Introduction to Environmental Biophysics, second ed., Springer, New York, 1998.
[33] J.L. Monteith, Evaporation and surface temperature, Q. J. R. Meteorol. Soc. 107 (1981) 1–27, http://dx.doi.org/10.1002/qj.49710745102.
[34] W.J. Stec, A.H.C. van Paassen, A. Maziarz, Modelling the double skin façade with plants, Energy Build. 37 (2005) 419–427, http://dx.doi.org/10.1016/j.enbuild.2004.08.008.
[35] R.S. Ulrich, R. Parsons, Influences of passive experiences with plants on individual well-being and health, Role Hortic. Hum. Well-being Soc. Dev. A Natl. Symp, Timber Press, Arlington, Virginia, 1992, pp. 93–103.
[36] G. Minke, G. Witter, Häuser mit grünem Pelz. Ein Handbuch zur Hausbegrünung, Verlag Dieter Fricke GmbH, Frankfurt, 1985.
[37] A. Miller, K. Ip, K. Shaw, M. Lam, Vegetation on Building Facades - Bioshader, Case Study Report (2007) http://documents.mx/documents/vegetation-and-building-facades.html.
[38] G. Pérez, L. Rincón, A. Vila, J.M. González, L.F. Cabeza, Energy efficiency of green roofs and green façades in mediterranean continental climate, Energy Convers. Manag. 52 (2011) 1861–1867 http://talon.stockton.edu/eyos/energy_studies/content/docs/effstock09/Session_11_1_Case studies_Overviews/102.pdf.
[39] R.G. Allen, L.S. Pereira, D. Raes, M. Smith, Crop Evapotranspiration - Guidelines for Computing Crop Water Requirements, (1998).
[40] M. Ottelé, The Green Building Envelope Vertical Greening, (2011).
[41] E.G. McPherson, Cooling urban heat islands with sustainable landscapes, Ecol. CityPreserving Restoring Urban Biodivers. (1990) 151–171 citeulike-article-id:2205597.
[42] N.H. Wong, A.Y. Kwang Tan, Y. Chen, K. Sekar, P.Y. Tan, D. Chan, K. Chiang, N.C. Wong, Thermal evaluation of vertical greenery systems for building walls, Build. Environ. 45 (2010) 663–672, http://dx.doi.org/10.1016/j.buildenv.2009.08.005.
[43] D. Watson, K. Labs, Climatic Design: Energy-efficient Building Principles and Practices, McGraw-Hill Book Company, New York, NY, USA, 1983.
[44] L. Kristanto, W.W. Canadarma, S.H. Nata, The effect of façade plant-shading on reducing indoor air temperature in medium-rise working area (a case study of architecture Student's studio in surabaya, Indonesia), in: 2005 world sustain, Build. Conf. Tokyo 2005 (27-29 Sept. 2005) 186–193. Tokyo.
[45] K. Ip, M. Lam, A. Miller, Shading performance of a vertical deciduous climbing plant canopy, Build. Environ. 45 (2010) 81–88, http://dx.doi.org/10.1016/j.buildenv.2009.05.003.
[46] N.A. Hendriks, G. Koers, Gevel Reeks 8-Groene Gevels, Sdu publishers, The Hague, The Netherlands, 2009.
[47] G. Pérez, L. Rincón, A. Vila, J.M. González, L.F. Cabeza, Behaviour of green facades in Mediterranean Continental climate, Energy Convers. Manag. 52 (2011) 1861–1867, http://dx.doi.org/10.1016/j.enconman.2010.11.008.
[48] B. Raji, M.J. Tenpierik, A. van den Dobbelsteen, The impact of greening systems on building energy performance: a literature review, Renew. Sustain. Energy Rev. 45 (2015) 610–623, http://dx.doi.org/10.1016/j.rser.2015.02.011.
[49] G. Pérez, J. Coma, I. Martorell, L.F. Cabeza, Vertical Greenery Systems (VGS) for energy saving in buildings: a review, Renew. Sustain. Energy Rev. 39 (2014) 139–165, http://dx.doi.org/10.1016/j.rser.2014.07.055.
[50] N. Kingsbury, N. Dunnett, Planting Green Roofs and Living Walls, Oregon, Timber Press, 2008.
[51] M. Köhler, Green facades - a view back and some visions, Urban Ecosyst. 11 (2008) 423, http://dx.doi.org/10.1007/s11252-008-0063-x.
[52] M. Manso, J. Castro-Gomes, Green wall systems: a review of their characteristics, Renew. Sustain. Energy Rev. 41 (2015) 863–871, http://dx.doi.org/10.1016/j.rser.2014.07.203.
[53] A. Lambertini, M. Ciampi, Giardini in Verticale, Florence (2007) https://www.ibs.it/giardini-in-verticale-libro-anna-lambertini-mario-ciampi/e/9781905216130.
[54] K. Perini, P. Rosasco, Cost–benefit analysis for green façades and living wall systems, Build. Environ. 70 (2013) 110–121, http://dx.doi.org/10.1016/j.buildenv.2013.08.012.
[55] M. Ottelé, K. Perini, A.L.A. Fraaij, E.M. Haas, R. Raiteri, Comparative life cycle analysis for green façades and living wall systems, Energy Build. 43 (2011) 3419–3429, http://dx.doi.org/10.1016/j.enbuild.2011.09.010.
[56] K. Perini, A. Magliocco, The integration of vegetation in architecture, vertical and horizontal greened surfaces, Int. J. Biol. 4 (2012) 79–91, http://dx.doi.org/10.5539/ijb.v4n2P79.
[57] K. Perini, M. Ottelé, E.M. Haas, R. Raiteri, Vertical greening systems, a process tree for green fa??ades and living walls, Urban Ecosyst. 16 (2013) 265–277, http://dx.doi.org/10.1007/s11252-012-0262-3.
[58] J. Coma, G. Pérez, A. de Gracia, S. Burés, M. Urrestarazu, L.F. Cabeza, Vertical greenery systems for energy savings in buildings: a comparative study between green walls and green facades, Build. Environ. 111 (2017) 228–237, http://dx.doi.org/10.1016/j.buildenv.2016.11.014.
[59] H.T. Odum, Environmental Accounting: EMERGY and Environmental Decision Making, John Wiley & Sons, Inc., 1996.
[60] R.M. Pulselli, F.M. Pulselli, U. Mazzali, F. Peron, S. Bastianoni, Emergy based evaluation of environmental performances of Living Wall and Grass Wall systems, Energy Build. 73 (2014) 200–211, http://dx.doi.org/10.1016/j.enbuild.2014.01.034.
[61] K. Perini, P. Rosasco, Cost–benefit analysis for green façades and living wall systems, Build. Environ. 70 (2013) 110–121, http://dx.doi.org/10.1016/j.buildenv.2013.08.012.
[62] B. Riley, The state of the art of living walls: lessons learned, Build. Environ. 114 (2017) 219–232, http://dx.doi.org/10.1016/j.buildenv.2016.12.016.
[63] W.J. Stec, Symbiosis of Double Skin Facade and Indoor Climate Installation, (2006) https://repository.tudelft.nl/islandora/object/uuid:360242c8-c1e6-4be5-bdc0-521d9238b1be?collection = research , Accessed date: 30 May 2017.
[64] M.M. Davis, S. Hirmer, The potential for vertical gardens as evaporative coolers: an adaptation of the 'Penman Monteith Equation', Build. Environ. 92 (2015) 135–141, http://dx.doi.org/10.1016/j.buildenv.2015.03.033.
[65] H. Kaase, A. Rosemann, Solarstrahlung und Tageslicht (Bauingenieur-Praxis, Band 1), Ernst & Sohn, 2018.
[66] B. Blocken, J. Carmeliet, The influence of the wind-blocking effect by a building on its wind-driven rain exposure, J. Wind Eng. Ind. Aerodyn. 94 (2006) 101–127, http://dx.doi.org/10.1016/j.jweia.2005.11.001.
[67] M. Kottek, J. Grieser, C. Beck, B. Rudolf, F. Rubel, World map of the Köppen-Geiger

climate classification updated, Meteorol. Z. 15 (2006) 259–263, http://dx.doi.org/10.1127/0941-2948/2006/0130.
[68] KNMI - Koninklijk Nederlands Meteorologisch Instituut (Royal Dutch Meteorological Institute), Eindhoven, Langjarige Gemiddelden, Tijdvak 1981-2010, (2010) http://www.klimaatatlas.nl/tabel/stationsdata/klimtab_8110_370.pdf , Accessed date: 21 May 2017.
[69] H. Sneep, Greenwave Systems, (n.d.). http://greenwavesystems.eu/(accessed 4 November 2016).
[70] Wallflore Systems N.V., Wallflore®, (n.d.). http://wallflore.eu/(accessed 4 November 2016).
[71] B. Blocken, J. Carmeliet, On the accuracy of wind-driven rain measurements on buildings, Build. Environ. 41 (2006) 1798–1810, http://dx.doi.org/10.1016/j.buildenv.2005.07.022.
[72] P.M. Briggen, B. Blocken, H.L. Schellen, Wind-driven rain on the facade of a monumental tower: numerical simulation, full-scale validation and sensitivity analysis, Build. Environ. 44 (2009) 1675–1690, http://dx.doi.org/10.1016/j.buildenv.2008.11.003.
[73] M. Van Noordwijk, G. Brouwer, Kwaliteit van steenwol is eenvoudig te meten, Tuinderij (1983) 25–27.
[74] B. Blocken, J. Carmeliet, Spatial and temporal distribution of driving rain on a low-rise building, Wind Struct. Int. J. 5 (2002) 441–462, http://dx.doi.org/10.12989/was.2002.5.5.441.
[75] AHN (A Cooperation of: Provinces; Central Government; Water Authorities), Actueel Hoogtebestand Nederland, 2011, http://www.ahn.nl , Accessed date: 12 July 2017.
[76] G. Piccinni, J. Ko, T. Marek, T. Howell, Determination of growth-stage-specific crop coefficients (KC) of maize and sorghum, Agric. Water Manag. 96 (2009) 1698–1704, http://dx.doi.org/10.1016/j.agwat.2009.06.024.
[77] R. López-Urrea, F. Martín de Santa Olalla, A. Montoro, P. López-Fuster, Single and dual crop coefficients and water requirements for onion (Allium cepa L.) under semiarid conditions, Agric. Water Manag. 96 (2009) 1031–1036, http://dx.doi.org/10.1016/j.agwat.2009.02.004.
[78] P. Lazzara, G. Rana, The crop coefficient (Kc) values of the major crops grown under Mediterranean climate, Mediterr. Dialogue Integr. Water Manag. FP6 INCO-MED Funded Proj, 2010.
[79] P. Lazzara, G. Rana, The use of crop coefficient approach to estimate actual evapotranspiration: a critical review for major crops under Mediterranean climate, Ital. J. Agrometeorol. Ital. Di Agrometeorol. 15 (2010) 25–39.
[80] F. Orgaz, M.D. Fernández, S. Bonachela, M. Gallardo, E. Fereres, Evapotranspiration of horticultural crops in an unheated plastic greenhouse, Agric. Water Manag. 72 (2005) 81–96, http://dx.doi.org/10.1016/j.agwat.2004.09.010.
[81] M.-T. Hoelscher, T. Nehls, B. Jänicke, G. Wessolek, Quantifying cooling effects of facade greening: shading, transpiration and insulation, Energy Build. 114 (2016) 283–290, http://dx.doi.org/10.1016/j.enbuild.2015.06.047.
[82] Eindhoven University of Technology, Overview Vertigo Department Built Environment, (2011) https://www.tue.nl/fileadmin/content/faculteiten/bwk/DDW_13/Overview_of_Technische_Universiteit_Eindhoven.jpg , Accessed date: 22 May 2017.
[83] meteoblue AG, Klimaat Eindhoven: Windroos, (2017) https://www.meteoblue.com/nl/weer/voorspelling/modelclimate/eindhoven_nederland_2756253 , Accessed date: 6 September 2017.